Tesi Doctoral

NMR IN DRUG DISCOVERY. FROM SCREENING TO STRUCTURE-BASED DESIGN OF ANTITUMORAL AGENTS

Ricard A. Rodríguez Mias

Departament de Química Orgànica

Facultat de Química

Universitat de Barcelona

Barcelona, Juliol 2006

3 KAHALALIDE F STRUCTURAL CHARACTERIZATION

Despite the recent combinatorial chemistry revolution, still around half of the drugs currently in use have a natural origin;[1] and in the particular field of cancer chemotherapies, some 67% of the effective treatments can be traced to a natural origin. Billions of years of evolution have yielded an astonishing variety of life forms on earth, tangled in a complex web of relations and spawned by interspecies competition over limited resources. From a chemical point of view these relations are usually mediated through a series of "non essential" biomolecules; secondary metabolites which in themselves are a reflection of the sheer number of interactions established throughout evolution.

In essence, nature has been engaged in a major combinatorial chemistry program for millions of years. No wonder it is difficult to surpass either in complexity or variety. This humbling lesson has been acknowledged for some time and traditional medicine has used the bioactive compound wealth, present in animals and plants, to treat nearly every human condition. During the last decades, a number of academic and non-academic efforts are trying to find some rational behind this folk knowledge, or even finding new applications to these treatments derived through millennia by trial and error; one such example is Chapter 2 of the present thesis, there some common Chinese traditional medicine treatments have been scrutinized to find new chemicals with anti-angiogenic activity.

Only with the advent of recent scuba diving techniques did the sea cease to be overlooked; and it is now regarded as a rich source of therapeutically useful compounds.[2-8] This is not surprising if one considers that water covers three quarters of the earth's surface and accounts for nearly 90% of its biosphere. Even beyond the opulence of the coral reef, the underwater world is a thriving environment; there, life has adapted and succeeded under the most demanding conditions; from the frozen poles to the heat sinks in the oceanic rift. Also the deep ocean, once considered to be a desert, has been recently rediscovered as a flourishing "rain forest" of unknown microorganisms.

The extremely crowded and competitive sea environment could account on its own for the variety of adaptations and life forms, and hence to a varied universe of secondary metabolites. But if one considers the hosts for these chemicals; we see most of them are produced by invertebrates such as sponges, tunicates and coelenterates, with limited skeletons and motility that have found the answers to their defense and feeding needs in their chemical arsenal. Another issue usually brought up to explain the high potency of marine origin compounds is the "dilution effect"; which basically states that in this underwater chemical war, weaponry gets diluted by sea water in its way to the target and thus only the most effective chemicals would survive the evolution sift. But are these reasons brandished above enough to justify their metabolite diversity and range of activities? Recent observations suggests that these invertebrates are not fully responsible for the wide list of metabolites, rather micro organisms such as bacteria or fungi frequently encountered in permanent association with them would be accountable for these compounds. Faulkner and co-workers supplied the first evidences in their work localizing natural compounds in the associations of micro organisms-sponge. Later other groups have identified several sponge secondary metabolites produced by symbiotic bacteria. [9] In this picture we could see tunicates, coelenterates and sponges as living fermentors; hiring the skills of symbiont mercenary bacteria in this particular chemical warfare.

Several decades of underwater exploration have produced a number of active compounds with activities ranging from antifungal, antiviral, anti-inflammatory or antibacterial. However the most populated class is that of antitumoral and cytotoxic compounds.[1, 3] This is probably a direct consequence of the early bioactivity guided isolations, and also due to the priorities imposed by funding organisms; although one

could also argue that there is a biological sense in the prevalence of cytotoxic activity in marine origin metabolites.

Whatever the reason may be, there is a long list of compounds with antitumoral activity that through the years have reached clinical trials, with differing fates.[2] Some of these agents, such as Didemnin B,[10, 11] turned out to be too toxic or their mechanism of action too unspecific to be approved by the regulatory agencies and were either dropped or underwent medicinal chemistry programs to improve their toxicity profiles. On the other hand compounds such as dehydrodidemnin B (Aplidine) [12] or ecteinascidin 743(Yondelis)[11] -a tunicate derived compound as well-, seem to present better selectivity towards tumor cells and are currently in phase II clinical trials for various cancers. The first generation of marine derived antitumoral drugs is expected in the following years, and due to the improved screening methodologies, a large number of compounds will certainly enter clinical trials with better success rates.

3.1.1 KAHALALIDE F

Kahalalides are a diverse family of peptides isolated from the sacoglossam mollusk *Elysia rufescens* and from an alga present in the mollusks diet: *Bryopsys sp.* [13] The family includes a variety of cyclic (Kahalalide A-F,K,O) [14, 15] and acyclic skeletons (Kahalalide H-J) [16], but its most relevant member is Kahalalide F. The latter exhibits an interesting cytotoxic activity against several solid tumor cell lines [17] and is currently in phase II clinical trials for melanoma, lung and prostate cancers. Anti-infective activity against several bacteria, viruses and fungi has also been described for Kahalalide F, and could also find application in the treatment of opportunistic infections related to AIDS.

#	residue
1	5-MeHx
2	D-Val
3	Thr
4	Val
5	D-Val
6	D-Pro
7	Orn
8	D-AlloIle
9	D-AlloThr
10	D-AlloIle
11	D-Val
12	Phe
13	Z-DhB
14	Val

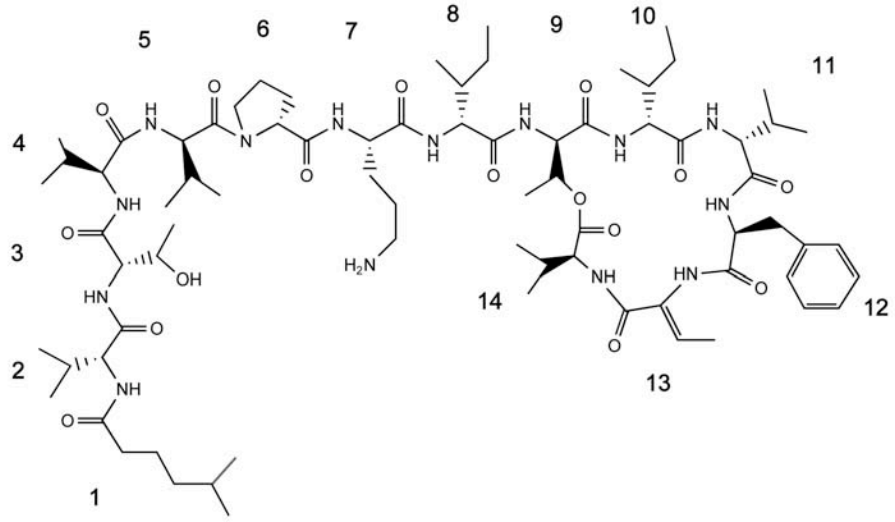

Figure 66 Kahalalide F sequence, chemical structure and numbering convention used throughout the current thesis.

Kahalalide F was first isolated by Hamman and Scheuer in 1993,[18] and its primary sequence established to contain 13 amino acids and a 5-methylhexanoic acid. The amino acids comprise several non-proteinogenic modifications such as reversed chirality, ornithine, $\alpha-\beta$ dehydro aminobutyric acid ((Z)-DhB), and the N-termini acylation with the 5-methylhexanoic acid. Another remarkable modification is the lactone

formed between the C-terminus of the peptide sequence and D-AlloThr 9 side chain, this depsipeptidic bond yields a 19-membered cycle, which has demonstrated crucial for the activity of the molecule as compared to its linear counterpart Kahalalide G.[14]

Independent works from Scheuer[14] and Rinehardt [19] set out to determine Kahalalide F absolute stereochemistry; their respective outcomes disagreed on the chirality of Val 5 and Val 4. The conundrum was unambiguously resolved by the synthetic work performed in our laboratory;[20] there, both diastereoisomers where synthesized and compared to the isolated natural product. Chromatographic retention time, NMR spectra, and biological activity for each isomer resolved the stereochemistry for Val 5 and Val 4, D and L respectively as shown in Figure 66

Kahalalide F Mode of Action (MOA) remains largely unknown, and so far no definite molecular target has been related to its activity. KF cytotoxic effects are exerted upon a variety of cell lines (kidney, prostate and breast among other) via an oncosis type cell death, inducing dramatic changes in sub cellular architecture and organelles. Swelling and vacuolization readily follow KF treatment, but damage to lysosomes, mitochondria, endothelial reticulum and plasma membrane are also observed. In contrast, DNA doesn't seem to be its target, and as expected for an oncosis type cell death it is not dependant on caspases nor on any other pro-apoptotic proteins.[17, 21]

At a molecular level, KF has been suggested to affect EGFR signaling pathway, crucial for cellular proliferation and differentiation. This hypothesis has been pursued by Jaanmat et al.[22] demonstrating increased sensitivity to KF by cells over expressing a certain type of EGF-receptor (ErB-3). According to their work KF effect on ErB3 would alter Akt (Protein Kinase B) phosphorylation and hence activate a necrotic-type cell death.

It is clear though, that KF displays a novel mechanism of action compared to other anticancer drugs; usually these induce apoptosis through DNA damage, activation of membrane death receptors or alterations on the cytoskeleton. In this sense Sewell et al. have explored KF's ability to permeate membranes on several tumor cell lines with different resistance profiles to the drug.[23] Their findings suggest that KF sensitive cells are more prone to permeate molecules in a wide range of masses, from propidium iodide (649 Da) to annexin V (35 KDa); the authors compare KF's permeation ability to maitotoxin another cytotoxic peptide that in contrast to ours, apart from membrane permeation is also capable of blocking calcium channels. To the light of these findings they propose a mechanism for KF similar to other cytotoxic compounds, or even a number of antibacterial peptides [24, 25]; with particular affinity towards lipidic bilayers and the ability to affect their integrity through various mechanisms. This seems a plausible explanation to the major effects KF has on cellular organelles, or its broad spectrum of activities.

Such lack of knowledge on KF's molecular target jeopardizes the long-term development of the compound as a drug. In fact, the possibility that toxic side effects for KF show up in late clinical phases has fostered the search for analogues with improved toxicology profiles. In this sense, the structural characterization of the compound should be able to guide the search for new active compounds or even shed some light on the mode of action and target. For this reason we intend to structurally characterize Kahalalide F under various conditions using NMR spectroscopy.

3.2 PRELIMINARY STUDIES IN DMSO AND H20

In this section we will explore several NMR parameters (see Introduction) for Kahalalide F in the search for structural preference evidences in two standard sample preparations: water and DMSO. Short linear peptides rarely show any definite structure and only in the best cases certain conformational preference may be inferred; this is not the case for small cyclic peptides or depsipeptides for which the cyclization largely limits the accessible conformational space. For this reason and keeping in mind the Kahalalide F "architecture" we anticipate some degree of structure although mainly in the macro-cyclic moiety.

3.2.1 DIMETHYLSULFOXIDE

The previously described assignment protocol [26] (NOESY, TOCSY 2D homo-correlation experiments) was performed for a 6mM Kahalalide F sample at 800MHz, and all peptide resonances were successfully identified. Later a series of mono-dimensional ^{1}H experiments were recorded at various temperatures in order to determine temperature coefficients for the peptide amides; the same ^{1}H experiments also allowed us to obtain $^{3}J\alpha N$ coupling constants.

The above data is summarized in Figure 67, together with relevant nOe cross peaks observed in the 2D ^{1}H NOESY experiment with 300 ms mixing time.

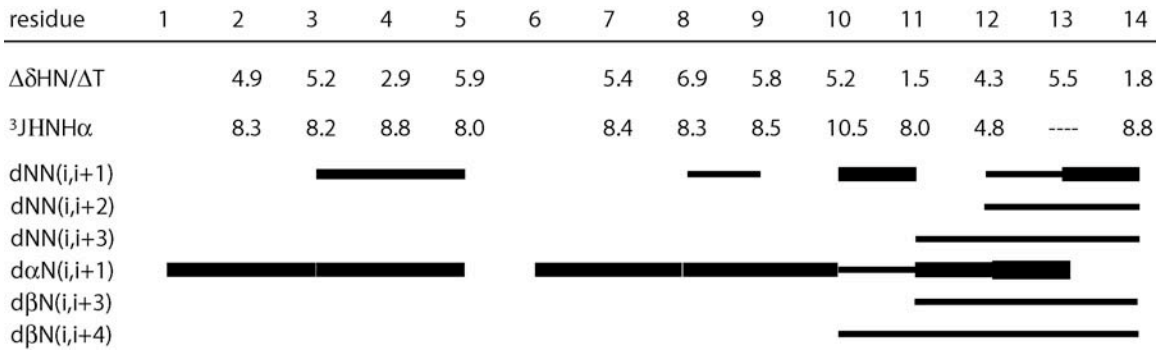

Figure 67: NMR derived data for Kahalalide F in DMSO-d6: temperature coefficients (ppb/K), $^{3}J_{\alpha N}$ (Hz), and relevant nOes (intensity is proportional to bar thickness).

In DMSO, most temperature coefficients ($\Delta\delta HN/\Delta N$) for KF's amides fall beyond the mentioned 4 ppb/K threshold; this suggests that the amides are exposed to the solvent. Three exceptions to this trend are observed along the sequence: amides 11 and 14 in the macro-lactone, and amide 4 in the N-terminus tail. The former is not surprising given the limited conformational freedom imposed by the cycle, and could be seen as an evidence for the presence of two trans-annular hydrogen bonds in this part of the molecule. The latter value, 2.9 ppb/K for valine 4, is remarkably low compared to its neighboring exposed amides, and could be an indication of certain structural preference in this region.

We observe a similar scenario for $^{3}J_{\alpha N}$ scalar coupling values, most of these coupling constants fall around 8.4 Hz, which according to tabulated values –extracted from protein databases- corresponds to amides in an anti-parallel β-sheet conformation. Nevertheless, structural interpretation of this data is complicated

especially for flexible molecules, where values between 6.3-9.5 Hz are often a result of averaging between various conformations. It is also in the C-terminus macro-cycle where exceptions to this pattern are observed, and extreme coupling constants such as 10.5 and 4.8 Hz are measured for D-allolle 10 and Phe 12 respectively. The presence of extreme $^3J_{\alpha N}$ coupling values has been identified as diagnostic for tight turn occurrence [27], and thus in this case would suggest two such bents; which in line with temperature coefficient observations could be stabilized by the detected hydrogen bonds.

On the other hand, the outcome for the NOESY experiment is typical of a non-structured molecule; dominated by sequential contacts particularly H_N-H_α, with the exception of the constraint C-terminus where contacts to i+2 or i+3 can be observed. In the rest of the molecule even H_{Ni}-H_{Ni+1} contacts are practically inexistent, and only observed for 3-4, 4-5 or weakly for 8-9 amides.

Putting together all these data, as anticipated we can draw two different pictures for Kahalalide F in DMSO. First the C-terminus, a highly restricted region, which encompasses two very protected and three exposed amides. These protected amides are probably engaged in some sort of hydrogen bond, and might be stabilizing two tight turns. This would explain the observed outlier $^3J_{\alpha N}$ values for amides 10 and 12, but also the typical β-sheet coupling constants for Val 14 and 11. The story is completed with the N-terminus section, which according to the data would be generally unstructured albeit the presence of N-N contacts, a slightly high $^3J_{\alpha N}$ (8.8 Hz) –compared to the neighboring amides- and a low temperature coefficient could indicate some preference towards a turn conformation around Val 4.

3.2.2 WATER

As for DMSO, we carried out the same analysis for the peptide in unbuffered water. Kahalalide F was dissolved in 9:1 H_2O:D_2O water to a 2mM concentration and the same set of NMR experiments performed for this sample. Assignment, temperature coefficients and $^3J_{\alpha N}$ measurements were also determined under these conditions.

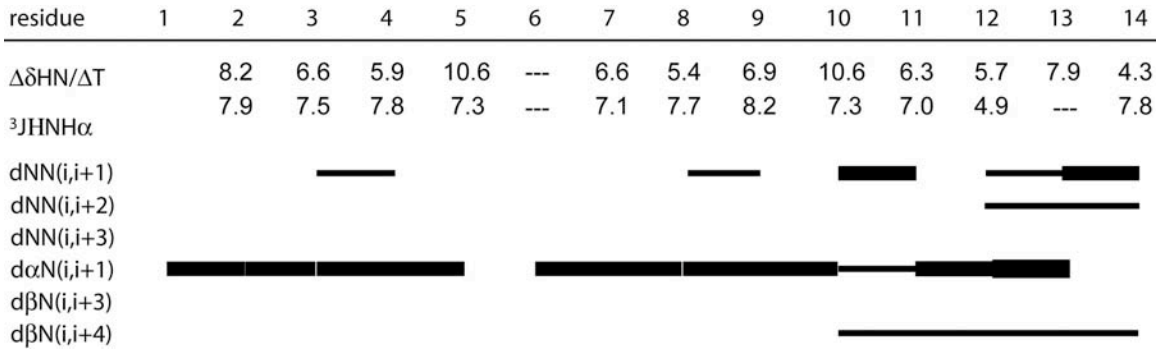

Figure 68 NMR derived data for Kahalalide F in D_2O: temperature coefficients (ppb/K), $^3J_{\alpha N}$ (Hz), and relevant nOes (intensity is proportional to bar thickness).

The same lack of nOe cross peaks -as observed for the DMSO sample- occurs under these conditions. Again, this is probably a consequence of Kahalalide F's adverse correlation time, combined with some degree of conformational flexibility. In fact the limited number of nOes is exacerbated by peptide solubility limitations, which do not allow us to use higher concentrations in order to boost cross-peak detection.

Somewhat related to the former solubility issue, an interesting observation was made with water Kahalalide samples. This is the detection of a sample "aging" process; which in the ^{1}H spectrum appears in the form of a time-dependant resonance broadening specially for amide signals (Figure 69). Similar effect can also be induced in the presence of TFE (20%), without any apparent precipitation occurring within the sample in either case.

Interestingly long treatments with TFA, followed by its removal via liophilization revert the process and produce a sample that is similar to a fresh one; particularly with respect to its ^{1}H NMR spectrum.(Figure 69) TFA treatments were introduced by Zagorski and collaborators [28] as an efficient pre-treatment protocol to disaggregate amyloidogenic proteins and achieve, for instance, water solubilization of the monomeric form for Aβ(1-42). This sort of treatment has become a standard procedure to achieve reproducibility in aggregation studies involving such "sticky" proteins. On the other hand, water-trifluoroethanol mixtures have been widely used in peptide NMR studies due to its ability to induce or enhance secondary structures to unstructured oligomers;[29] usually promoting alpha-helical motifs,[30] although β-turns have also been reported.[31] The current belief is that these effects are mediated by its mild denaturing properties, stemming from TFE hydrophobicity and hydrogen bonding capabilities, which tend to favor short hydrogen bonds and destabilize tertiary folds. In some instances these features have been seen to induce fibrillogenesis of certain proteins, particularly those with β-barrel folds. [32, 33]

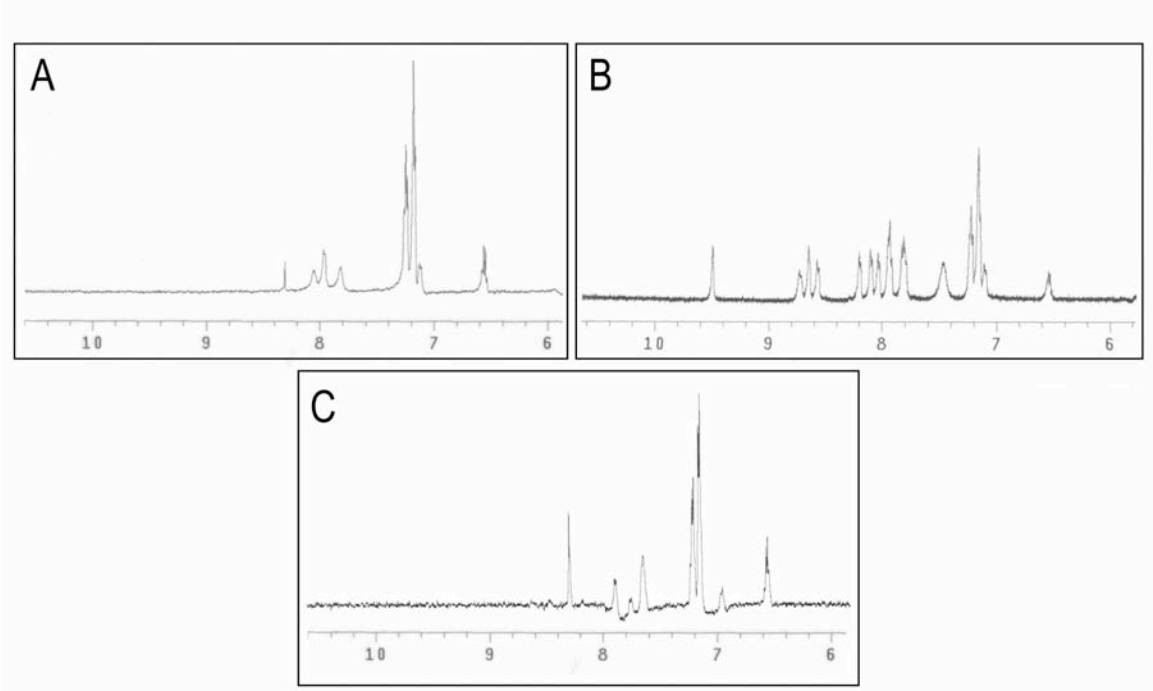

Figure 69: Amide region for 1H watergate experiments for 2mM Kahalalide F samples: A) in water after aging process occurs; B) in water "aged" sample after TFA treatment; C) in TFE/Water 2:8.

These observations are appealing indications that both, time and TFE could be triggering some sort of aggregation or supra-molecular organization process for Kahalalide F. For this reason, and in order to get further insight into the peptide solution species Transmission Electron Microscopy (TEM) was proposed. TEM has an outstanding ability to directly probe the state of a solution sample and for this, it is often used to

study protein oligomers and aggregates. Other applications include characterization of detergents and its micellar microstructures, which experience dramatic shape adjustments in front of environment changes such as counter ion nature, temperature and pH.[34, 35]

Experiments were performed for a TFE treated and a "monomeric" control (TFA treated) 10^{-5} M peptide sample. These were fixated, dried and negatively stained with a platinum replica to be later observed under the microscope. And indeed Figure 70 suggests we are probably before one of such systems. Kahalalide F experiences an apparent increase in its correlation time upon TFE treatment in the NMR experiment; which under the electron microscope appears as some sort of organization into thoroidal or "doughnut -like" micro-structures with a typical diameter of 20 nm. On the contrary TFA treated samples present amorphous clumps of peptide scattered throughout the grid.

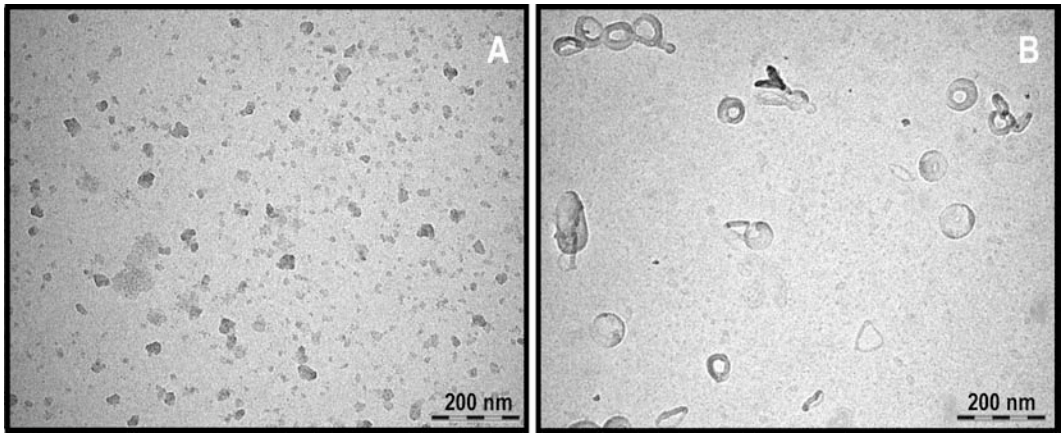

Figure 70: Cryo transmission electron microscopy pictures for 10^{-5} M Kahalallide F samples: A) TFA treated; B) water/TFE 8:2.

Similar organizations have been observed using TEM for ionic and anionic surfactants [34], suggesting that TFE and time could mediate a micellation phenomenon on the peptide, not surprising considering the amphipathic nature of Kahalalide F.

3.3 STRUCTURAL CHARACTERIZATION IN SDS MICELLS

The previous section has turned out to be exploratory, in the sense that we have tested two typical NMR sample preparations and tried to detect Kahalalide F structural propensities under these conditions. Unfortunately the result has not been satisfactory, and in either condition there does not seem to be any clear structural preference beyond the restricted C-terminus macro-cycle; which incidentally, seems to arrange analogously in both media. Solubility issues are partly responsible for such failed characterization in water; and in the case of DMSO, although certain evidences suggest some sort of turn preference in the N-terminus, there are no clear nOes to support the observations or an eventual structure calculation.

KF's mode of action remains largely unknown; nevertheless there appears to be some consensus on its membrane and organelle destabilizing effects. Given that its activity is somewhat circumscribed to a lipid or membrane environment, it seems only natural to explore our options for an eventual NMR study in membrane-like media; and to this aim we will dedicate the following section.

3.3.1 NMR STUDIES OF LIPID/PEPTIDE SYSTEMS

Biomembrane interactions are of utter importance in almost all biological processes. Cellular compartmentalization requires the existence of transport and signaling mediators, hence a number of important regulatory events take place at a membrane level: for instance, brain biochemistry heavily relies on various transmembrane receptors (GPCRs) and ion channels. In fact, due to the ubiquity of these membrane-bound proteins, it is not surprising that nearly 70% of drugs currently in the market target receptors of this type. [36]

Regrettably, size, composition and complexity of these systems hamper the use of solution NMR to characterize receptor structures or even their interactions with the membrane and/or other molecules. Here one has to turn to X-Ray crystallography in order to solve protein structures,[37] or solid state NMR (ssNMR) that has found a wide use to study antimicrobial peptides interacting with lipid bilayers, which often pose serious crystallization issues [38]. But aside from the particular biophysical technique, membrane morphology is still extremely complex; formed by a variety of sugars, phospholipids and proteins, without an homogeneous composition among the various phyla: bacteria, fungi, etc, but also between different tissue cells. As a result, studies in lipidic environments tend to be performed in membrane simplifications or mimics rather than the natural heterogeneous mixture.

In the attempt to supplant lipid bilayer, probably the simplest approach consists in trying to reproduce the physicochemical properties of the water-membrane interface. And this has been achieved with 1:1 chloroform/methanol mixtures, which produce a very similar dielectric environment as found in the membrane rim. Various trans-membrane protein domains have been structurally characterized under these conditions,[39, 40] although in some cases aggregation complicates peptide studies, and of course few full proteins maintain their activity in such conditions. In this direction, Rastogi et al. have gone a step forward and used aqueous chloroform/methanol mixtures to solve the structure of Translocation subunit c for ATP synthase. [41]

Compared to organic solvent mixtures, detergent micelles are more sophisticated models and are the most frequent membrane mimic used for solution NMR studies. Detergents are extremely amphipathic molecules, with a polar head and a long hydrophobic tail, and above a certain concentration they tend to aggregate in

water forming micelles. These spherical aggregates expose their hydrophilic heads to the solvent, and exclude water molecules from the hydrophobic interior; they are composed by a variable number of monomers depending on the detergents nature: e.g. around 60 for DPC or 85 monomers in the case of octylglucoside [42] [43] .The relatively reduced size of the detergent aggregates makes them amenable to solution NMR studies, and explains its wide application in the study of membrane interacting peptides such as the wide family of antimicrobial peptides.[38] Commercial availability of deuterated detergents is yet another reason for its predominance in the study of non-labeled membrane-interacting peptides. However the reduced micelle particle size often induces curvature effects on the interacting peptide, an artifact that would predictably not happen on flat phospholipid bilayers.

Bicelles are another step ahead in membrane mimicry,[44] discoidal bilayered aggregates typically composed by two kinds of phospholipids; which differ in their hydrophobic tail length (generally DHPC and DMPC). The longest of the phospholipids conforms the bicelle bilayer fraction while the shorter counterpart is located at the bicelle round edge. Thus, the particular ratio between phospholipids determines the geometrical parameters for the bicelle. These aggregates are larger in size than micelles, and find themselves at observation limit by solution NMR techniques if the molecule of study binds too tightly. Nevertheless there are some examples of structural studies performed with bicelle-interacting peptides [45], there the mentioned curvature distortion present in micelles is no longer an issue. Despite the limitations, these systems have had a major impact on the structural biology field; Bax and collaborators [46] demonstrated it was feasible to use the natural bicelles tendency to align under a magnetic field to enhance protein anisotropy and achieve residual orientation for the latter. This residual alignment on the protein could further be used to get structural information in the form of residual dipolar couplings (RDC), a type of long-range structural information largely complementary to the nOe that can also be introduced as constraints into structure calculations.

Vesicles and liposomes are spherical compartments of bilayered or multilayered phospholipids that usually enclose water; and among membrane models, are probably the closest one can get to the real thing. Unfortunately their size is again the limiting factor at least for solution NMR; not so for other biophysical techniques such as solid state NMR (ssNMR) or EPR. [38]

It is clear from the above rough overview, that there is a wide range of choices to simulate membrane environments. Nonetheless our system imposes several limitations: Kahalalide F is produced from chemical synthesis, and production with any other host than its natural sources (*Elysia rufescens* and *Bryopsys sp*.) has not been reported so far. Therefore, introduction of stable isotopes for the NMR characterization can only be achieved through chemical synthesis and would entail very high costs. Consequently we are doomed to natural abundance nuclei, and given the high concentrations required for all mentioned membrane mimics, the only viable choice is the use of deuterated alternatives. DHPC/DMPC bicelles, vesicles and liposomes are not available in their deuterated form, besides they have too large a correlation time and will most likely be unsuitable for our solution NMR studies.

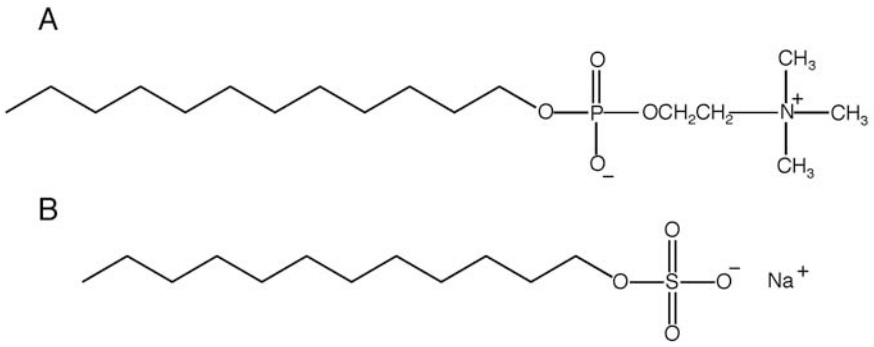

Figure 71: Chemical formula: A) Dodecyl-Phosphocoline (DPC), B) Sodium Dodecyl-Sulfate (SDS).

As opposed to bicelles, both organic solvents and detergents, such as SDS or DPC, (Figure 71) are available in their deuterated forms; moreover in both media peptides are usually amenable to solution NMR techniques. However, organic solvent mixtures are probably too simple as membrane models; also given the poor results obtained in the previous sections with DMSO and dispite of its higher dielctric constant compared to methanol/choroform mixtures, it is probably wiser to test a more sophisticated model.

Both SDS and DPC are widely used in solution NMR studies, and both have a similar aliphatic chain (dodecyl) the difference however lays in the polar group, and while SDS's sulfate group is negatively charged the phosphochloline head in DPC is zwitterionic. This explains certain properties for SDS, such as its higher critical micellar concentration or its strong denaturing behavior towards proteins. DPC on the contrary is a milder denaturing agent, moreover, its phosphocoline group is a very abundant polar group in natural lipid bilayers. From such properties, it would seem that DPC is superior to SDS as membrane mimic, but some authors suggest a use of mixed micelles in order to modulate the surface charge content.[47, 48] If we now consider our particular case, the presence of one ornithine in Kahalalide F as its only charge advises towards incorporation of net negative charges on the micelle surface in order to improve peptide/micelle solubility; also, in terms of commercial availability and cost, sodium docedylsulfate seems to fit best our needs. From a biological perspective, it is interesting to note that membrane composition in tumor cells has been reported to differ from their healthy counterparts, particularly the presence of higher ratios in negatively charged phospholipids has been noted by several authors [49] and could well be part of the reason behind Kahalalide F's selectivity, along with a justification for our particular detergent choice.

3.3.2 KAHALALIDE F SOLUBITILY IN SDS MICELLS

Once SDS was chosen as our membrane surrogate, we decided to explore different sample conditions namely peptide/SDS ratio, and for this purpose several samples were prepared. Peptide concentration was kept constant to 0.5mM and increasing amounts of SDS were added from a concentrated detergent stock. In this way peptide ^{1}H spectra were acquired for samples containing 0, 1, 3, 5, 10, 50 and 100 mM d_{25}-SDS.

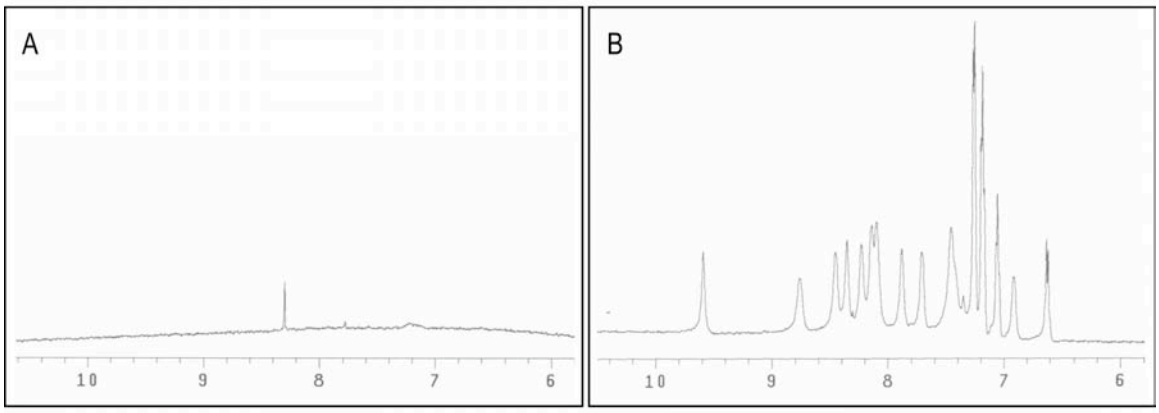

Figure 72: ^{1}H NMR spectra amide region for 0.5mM Kahalalide F samples: A) 1mM SDS; B) 10mM SDS in water.

Upon 1 mM SDS addition into the sample, this became turbid probably due to peptide solubility problems as it was later confirmed in ^{1}H NMR spectrum (Figure 72). This same behavior continues until SDS concentration reaches 5 mM, at this point the overall sample condition improves dramatically, and the ^{1}H NMR confirms that the peptide has been redissolved (Figure 72). Beyond 10 mM SDS no important changes occur on the spectra a part from pH related shifts on amide protons.

Peptide insolubility has previously been described in the presence of low SDS concentrations, especially below its c.m.c (critical micellar concentration). Below this concentration SDS does not form stable aggregates and its hydrophobic tail will likely pack with hydrophobic parts of the peptide triggering its precipitation. The concentration at which stable micelles are formed in water, is a characteristic value for each detergent, and is very sensitive to ionic strength and counter-ion nature and temperature. In our case, and according to the literature, SDS reaches this critical value around 5-8mM [50]; this is consistent with our titration results. Thus, below SDS c.m.c, Kahalalide F precipitates and only above this concentration does it resolubilize. It would seem then that stable micelles are required for the peptide to remain in solution, which in turn implies some sort of peptide-micelle assembly.

Further evidences of interaction between peptide and detergent aggregates are found upon ^{1}H NMR spectra inspection. In general, peptide signals become broadened in the presence of SDS micelles, this can probably be attributed to the apparent increase in size suffered by KF upon interaction with detergent aggregates. These particles vary in their number of SDS molecules depending on ionic strength, counter-ion etc; but under low salt conditions they are believed to accommodate from 60 to 100 monomers. Considering that each micelle contains a single peptide molecule we can agree that the molecular weight of one such micelle-peptide particle would compare to a 10 KDa protein. Thus, line-broadening issues are not surprising, even so as to impair $^{3}J_{\alpha N}$ couplings measurement for most amides (see Figure 73).

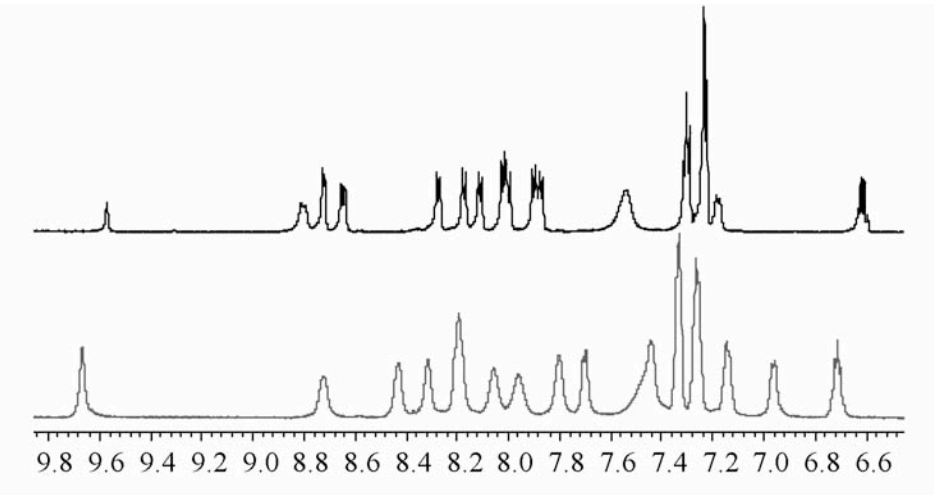

Figure 73: Amide region for 1H experiments for A) 2mM Kahalalide F in water and B) 6mM sample in water/SDS 150mM.

Already prior to the detailed resonance assignment we can advance important chemical shift differences for Kahalalide F resonances in water compared to water/SDS medium; this is particularly relevant for non-exchangeable resonances, less subject to pH changes. In this sense Phe 12 aromatic protons experience remarkable shifts and while in water $H_{2,6}$ $H_{3,5}$ and H_4 protons appeared clustered in two multiplets at 7.3 and 7.2 ppm, in water/SDS they are completely differentiated. This is very likely due to drastic changes imposed to Phe 12 aromatic ring by micellar hydrophobic environment, yet another hint of the peptide immersion in the detergent aggregates.

Taken together, all these data strongly support our hypothesis of Kahalalide F interacting with SDS micelles, and as an extension with biomembranes. This is not surprising since its chemical structure and macroscopic behavior in water already anticipated certain amphiphilicity: Kahalalide F is largely hydrophobic, mainly composed by aliphatic amino acids and notably its N-terminus acylation, the only exceptions are Thr 3 hydroxyl group and a charge –Orn 7- placed at the sequence geometric centre; in essence a bifid detergent molecule.

3.3.3 NMR ASSIGNMENT

A 6mM sample was prepared for Kahalalide F, and 150 mM d_{25}-SDS were added to the 9:1 H_2O/D_2O mixture. This particular peptide/SDS ratio was chosen to minimize the number of peptide copies per micelle particle in order to avoid eventual interactions between different KF molecules.[51] With such ratio, and estimating 60 SDS monomers per particle, each detergent aggregate would be shared roughly by two Kahalalide molecules.

The aforementioned Wütrich et al. [26] methodology was used to completely identify peptide resonances at 283 K (Table 3) and at 298 K. Figure 74 corresponds to a superposition of the fingerprint region for 2D-TOCSY and NOESY experiments used in the assignment process.

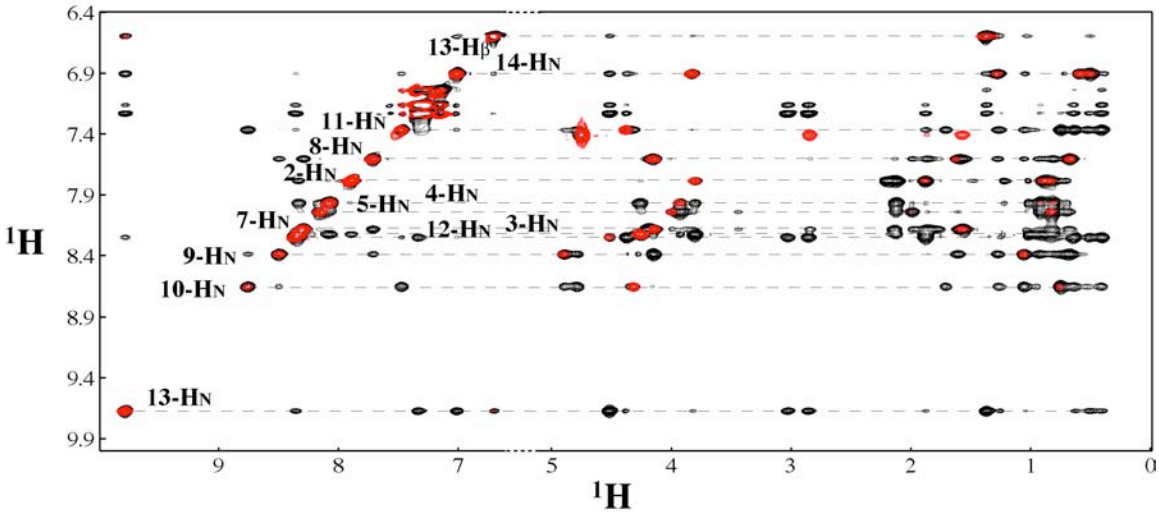

Figure 74: Overlay of ^{1}H 2D homocorrelation experiments finger print regions for a 6 mM Kahalalide F sample: 2D-TOCSY τ_m=80ms (red) and 2D-NOESY τ_m=200ms (black).

	Residue	HN	Hα		Hβ		other
1	MeHx		2.16	2.21	1.50	1.25	1.22 Hγ 1.01 1.22 Hδ$_1$ 0.73 Hδ$_2$ 0.73 Hε
2	D-Val	7.84	3.83		1.89		0.90 0.84 Hγ
3	Thr	8.26	4.27		4.29		1.02 Hγ
4	Val	8.01	3.94		2.13		0.92 0.82 Hγ
5	D-Val	8.08	4.02		2.00		0.83 Hγ
6	D-Pro		4.21		2.15	1.96	1.79 1.85 Hγ 3.45 3.86 Hδ
7	Orn	8.23	4.16		1.58	1.87	1.58 Hγ 2.85 Hδ Hε
8	D-AlloIle	7.64	4.15		1.64		1.28 0.93 Hγ$_1$ 0.68 Hγ$_2$ 0.71 Hδ
9	D-AlloThr	8.43	4.78		4.92		1.07 Hγ
10	D-AlloIle	8.70	4.33		1.72		1.25 0.99 Hγ$_1$ 0.76 Hγ$_2$ 0.76 Hδ
11	D-Val	7.40	4.39		1.90		0.66 0.42 Hγ
12	Phe	8.30	4.52		3.03	2.88	7.17 H$_{2,6}$ 7.24 H$_{3,5}$ 7.04 H$_4$
13	Z-DhB	9.69			6.60		1.37 Hγ
14	Val	6.93	3.83		1.28		0.60 0.52 Hγ

Table 3: Resonance assignment table (ppm) for 6 mM Kahalalide F in water/SDS 150 mM sample.

A first qualitative inspection of the NOESY spectrum reveals a large number of intense nOe cross-peaks; with the same sign as the diagonal and a remarkable intensity; as it corresponds to large molecule. Interestingly the number and intensity of nOes exceeds those found in either water or DMSO; moreover this number seems to augment for experiments recorded at 283 K compared to those acquired at r.t. This can probably be attributed to an increase in sample viscosity or even a temperature dependant micelle enlargement. This temperature effect on the overall peptide correlation time can also be observed in the $^{3}J_{\alpha N}$ constants, such coupling constants are generally inaccurate at 298 K as already mentioned due to SDS, but at 283 K they become practically not measurable for any amide. (Figure 75)

In general, the amount, sign and intensity of nOe cross-peaks seem to support the formation of a high-molecular weight mixed micelle between SDS detergent molecules and Kahalalide F.

3.3.4 TEMPERATURE COEFFICIENTS

In the same manner as in preceding sections, mono-dimensional ^1H spectra were acquired at different temperatures, from 283 to 313 K, to produce the array shown in Figure 75. The resonance assignment sample -6 mM peptide/150 mM SDS- was used for this purpose, and the chemical shift slope with temperature measured for amide protons (Figure 76).

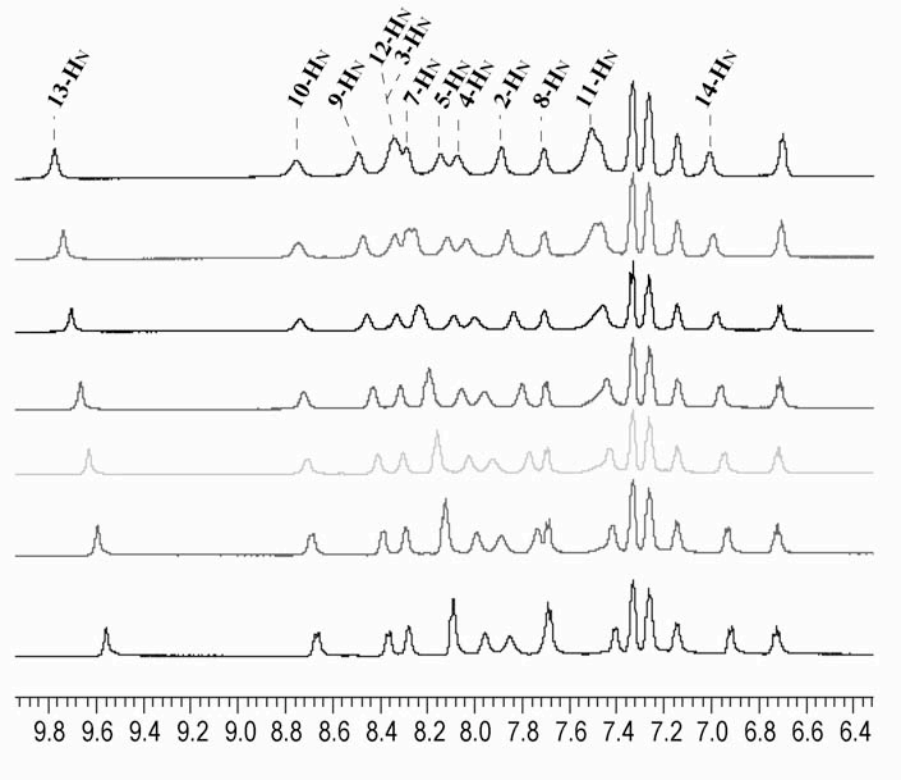

Figure 75: ^1H Watergate experiments for 6mM Kahalalide F in water/SDS 150mM at different temperatures: 283, 288, 293, 298, 303, 308, and 313 K (from top to bottom)

Traditional threshold values for temperature coefficients have been set around 7 ppb/K for solvent exposed random coil amides, and values below 4 ppb/K have been considered as structurally relevant in aqueous medium.[52] Nonetheless, in our particular medium this could not hold true, since SDS micelles could have an effect on temperature coefficient measurements beyond structure stabilization. In fact, water is inherently excluded from micelle's interior, and therefore this environment is probably closer to a protein hydrophobic core or to CH_2Cl_2 than to hydrogen bonding solvents such as DMSO or H_2O. Similarly, another consideration would deal with amide solvent accessibility, and its mechanistic implications to temperature coefficient measurements. In the particular case of deeply buried or unexposed amides, hydrogen bonding with the solvent may rarely occur; hence temperature effects on such hydrogen bond network and its associated perturbations on amide chemical shifts would not occur either. This is true for tightly packed protein cores or cyclic peptides where structure stiffness may hinder solvent access almost completely, but how much of this applies to the interior of a detergent micelle?

Spyracopoulus et al. [53] have addressed this questions by measuring temperature coefficients for a series of tailored amides varying in their aliphatic content. They noted minor increases on temperature coefficients upon micelle insertion; this enhanced amide "exposedness" was attributed to the lack of solvent molecules with which to hydrogen bond in the micelle's interior. According to this it still seems safe to associate low temperature coefficients with stable hydrogen–bonding, and thus for the sake of convenience we will stick to the 4ppb/K convention.

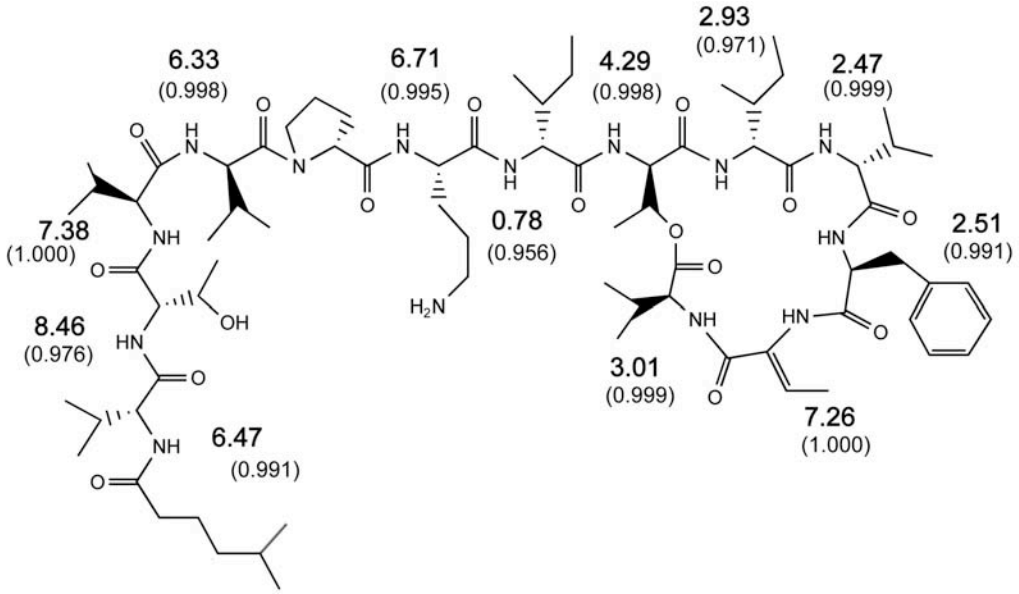

Figure 76: Kahalalide F chemical structure, temperature coefficients (ppb/K) are plotted for each amide and in brackets their corresponding linear regression coefficient (R^2).

Overall Kahalalide F shows a wide range in temperature coefficient values. Amides within C-terminus depsi-peptide macro cycle show particularly low values, and nearly all of them fall below the 4ppb/K threshold. This can be explained by the presence of hydrogen bonds within the macro lactone, although it is highly unlikely that so many amides are involved in such interactions for so small a cycle. Consequently another plausible explanation could be that some of these amides are not easily accessible to the solvent due to the tightly packed nature of the lactone. The only exception to this pattern is dehydro amino acid's amide with a 7.26 ppb/K coefficient; the reason probably being related to the unusual electronic properties of its side chain. The electron-withdrawing propensity of the $\alpha-\beta$ double bond in the side-chain most likely lowers the amide's pKa, as a result this becomes more prone to chemical exchange with water protons, thus chemical exchange probably dominates the unexpectedly high temperature coefficient.

Conversely, the situation changes when we analyze temperature coefficients for the N-terminus tail. Here most coefficients fall around the 7 ppb/K consensus random coil value, with the exception of D-alloThr 9, - the last exo-macrocyclic amide- barely above the "hydrogen-bonding" threshold. Again, the latter can probably be explained in terms of limited solvent accessibility due to the neighboring cycle. The other remarkable outlier is D-allo-Ile 8, this amide has by far the lowest coefficient throughout the peptide and remains nearly unaffected by temperature as seen in the 1D spectra array Figure 75. This fact strongly

supports involvement of this amide in a hydrogen bond, and may have some structural implications regarding Kahalalide F's tail segment, which in the previous media appeared largely random coil.

3.3.5 AMIDE EXCHANGE RATES

Tightly packed folds or secondary structure motifs such as those found in proteins, are rich in hydrogen bonds; crucial for their thermodynamic stability but also guiding many folding reaction. Evidence for hydrogen bond formation has traditionally been sought in amide-water proton exchange rates; where those protons protected from solvent exchange are identified as hydrogen bond donors, or otherwise buried in the protein core. Not surprisingly, there is a wealth of literature reporting the use of exchange rates as a source of structural information for various systems including: soluble proteins, amyloid fibrils or even protein folding and dynamics.[54, 55] On the contrary, this kind of data is sparser for small peptides since they are often unstructured and is harder to obtain; however there still are examples with micelle bound peptides, for which the detergent provides certain protection through structure induction or solvent exclusion.[56, 57] Such is the idea in this section: to perform solvent exchange rate measurement expecting some micelle enhanced protection for Kahalalide F.

For protein/peptide systems, rather than using the amide exchange rate by itself, structural analysis is most often performed in terms of amide protection factor (Equation 6); this PF compares the amide exchange rate for the amide within its protein environment, and its calculated exchange rate in a random coil model. In this way primary sequence inductive and steric effects are ruled out, and only structural effects are taken into account.[58]

$$P = k_{rc} / k_{prot}$$
$$k_{rc} = k_{(acid)} + k_{(basic)} + k_{(water)}$$
$$k_{rc} = k_{A,ref}(A_L \times A_R)[D^+] + k_{B,ref}(B_L \times B_R)[OD^-] + k_{w,ref}(B_L \times B_R)$$
$$\log k_{(acid)} = \log K_{A,ref} + \log A_L + \log A_R - pD$$
$$\log k_{(basic)} = \log K_{B,ref} + \log B_L + \log B_R - pOD$$

Equation 6: Equations used in Protection Factor calculation; A_L,A_R,B_L,B_R, $K_{A,ref}$ and $K_{B,ref}$ are obtained as described by Bai and collaborators.[58]

Performing this type of measurements in a molecule like Kahalalide F has its overheads. These difficulties stem out from the fact that our peptide is not fully composed by proteinogenic amino acids, and also as a consequence of using an SDS/water mixture.

With regard to the first issue, calculation of random coil exchange rates for an amide involves the use of several tabulated values as we can see in formulas (Equation 6), this L and R tabulated values correspond to amino acids in *i-1* and *i* respectively. The problem is that tabulated values are only available for natural amino acids, since most of this studies are performed for proteins; consequently we will not be able to correctly determine the random exchange rates for Z-Dhb, ornithine or for those amides at *i-1* to depsipeptide or N-terminus moiety.

On the other hand, a second limitation may prove important when it comes to the structural interpretation of the data. As said, protein core amides, although seldom found as non-hydrogen bonded, will expectedly have low exchange rates due to reduced solvent accessibility. A similar argument may apply for amides deeply embedded in SDS micelles; in fact, under such circumstances it could be difficult to differentiate between an amide intervening in a hydrogen bond or one with a preference for the micelle's core. In this sense Spyracopoulus et al. [53] observed exchange rate value reduction upon SDS solubilization for a set of model amides.

Although there exist numerous methods to measure amide exchange rates,[55] probably the most straightforward NMR method consists in dissolving the protein or peptide in D_2O and measuring the decay of its exchangeable protons with time. Adjusting this decay to an exponential function will yield the exchange rate values. The particular NMR experiment used can either be mono or 2D, the choice will depend on the availability of labeled peptide, signal overlap and most importantly the time range required for complete proton exchange.

A 2 mM Kahalalide F sample was dissolved in 50 mM SDS/D_2O, readily introduced in the spectrometer and a series of ^1H Watergate experiments –evenly spaced 5min in time- acquired. For the sake of consistency peptide/SDS ratio was kept similar to the assignment and temperature coefficient experiments; also, in order to reduce as much as possible proton exchange the experiment was recorded at 283 K. Following acquisition, each experiment was processed, the amide peaks assigned and its intensity measured; later this value is plotted versus time and the curves adjusted to an exponential function (Figure 77).

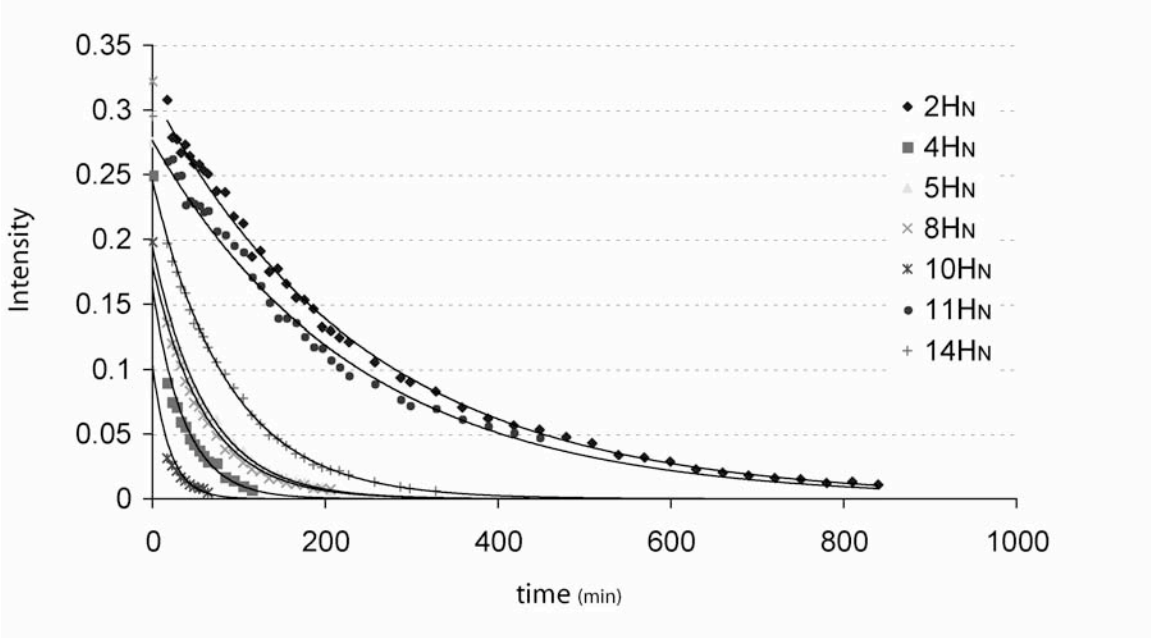

Figure 77: H_2O/D_2O exchange curves for Kahalalide F amide protons in water/SDS 150 mM. Amide intensity in ^1H NMR experiment versus time at which experiment is acquired are represented and adjusted to exponential function.

As described by Bai and collaborators[58] K_{rc} were calculated for KF amides, and used together with the experimental rates to obtain protection factors (Equation 6). However, due to the unusual amino acid

composition in our peptide we have to point out several assumptions throughout random coil exchange rates calculations: N-terminus acylation was considered as an isoleucine, ornithine as an arginine, and Z-Dhb was equated to serine.

As we see in Table 4, water exchange rates were obtained for most of Kahalalide F amides, except for Thr3, Orn-7, alloThr9, Phe12, and Z-DhB13 that exchanged too fast to be measured. Measurement of these exchange rates would require other NMR experimental set up such as for instance experiments using saturation transfer.[55, 59] Still, with our set up we are able to provide a lower exchange rate threshold or a maximum Protection Factor for these fast exchanging amides.

residue	K_{obs} (min^{-1})	Amide	K_{rc} (min^{-1})	PF
2	4.10E-03	"Ile"-NH-Val	4.23E-02	10.3
3	5.00E-02	Val-NH-Thr	2.22E-01	4.4
4	2.70E-02	Thr-NH-Val	4.53E-02	1.7
5	1.63E-02	Val-NH-Val	1.40E-01	8.6
7	>5.00E-02	Pro-NH-"Arg"	2.49E-01	<5.0
8	1.68E-02	"Arg"-NH-Ile	1.11E-01	6.6
9	5.00E-02	Ile-NH-Thr	1.80E-01	3.6
10	4.97E-02	Thr-NH-Ile	1.06E-01	2.1
11	4.20E-03	Ile-NH-Val	4.23E-02	10.1
12	>5.00E-02	Val-NH-Phe	1.50E-01	<3.0
13	>5.00E-02	Phe-NH-"Ser"	9.69E-01	<19.4
14	1.15E-02	"Ser"-NH-Val	1.43E-01	12.5

Table 4: Kahalalide F amide exchange rates obtained from D_2O/H_2O exchange experiment (K_{obs}); random coli rates (K_{rc}) and protection factors calculated as calculated by Bai et al.[58] Where tabulated values were unavailable amino acids appear in quotes. For such calculations Ile, Arg, Ser tabulated values were used instead of the non-proteinogenic residues: Methylhexanoic Acid, ornithine and Z-Dehydroaminobutyric acid respectively. Where exchange rate could not be measured experimentally an upper limit for K_{obs} and lower Protection factor (PF) limit are given.

Comparison between observed exchange rates and calculated protection factors seems to provide similar information. Both parameters agree in amides 2, 11, 14 and 5 being the most protected; although the exact order –especially for the first three- does not match. Protection factors are supposed to account for electric and steric sequential effect; in our case however, given the relatively low protection provided by the peptide, these effects are not mere corrections and in some instances become as important as the observed exchange rate itself. For this reason, interpretation of the raw observed exchange rates is risky and calculation of Protection Factors is more than encouraged, inaccuracies notwithstanding.

Among the approximations used to determine protection factors probably the least audacious are those for methylhexanoic N-terminus and ornithine, in both cases substitutions are reasonably similar in their steric and electric nature and the obtained values will probably make good guesses. Calculation of random coil exchange rates for amides 13 and 14 arise more concerns, especially since Z-DhB's substitute (serine) will likely underestimate the electron-withdrawing effects induced by the $\alpha-\beta$ insaturation; this will especially affect the protection factor accuracy for amide 13. In fact, the protection factor calculated for this amide is the highest, yet its exchange rate is too fast for our experimental set up; again, this could be a direct consequence of its abnormally acidic pKa. With respect to Val 14 K_{rc} calculation, inaccuracies will not be as severe, especially since the effects of Z-DhB are not so much electronic as they are steric and, in terms of side chain volume, serine resembles closely the dehydro amino acid. Also, for this particular case the presence of the ester bond has been omitted from the process, a fact that will certainly introduce some error in this protection factor.

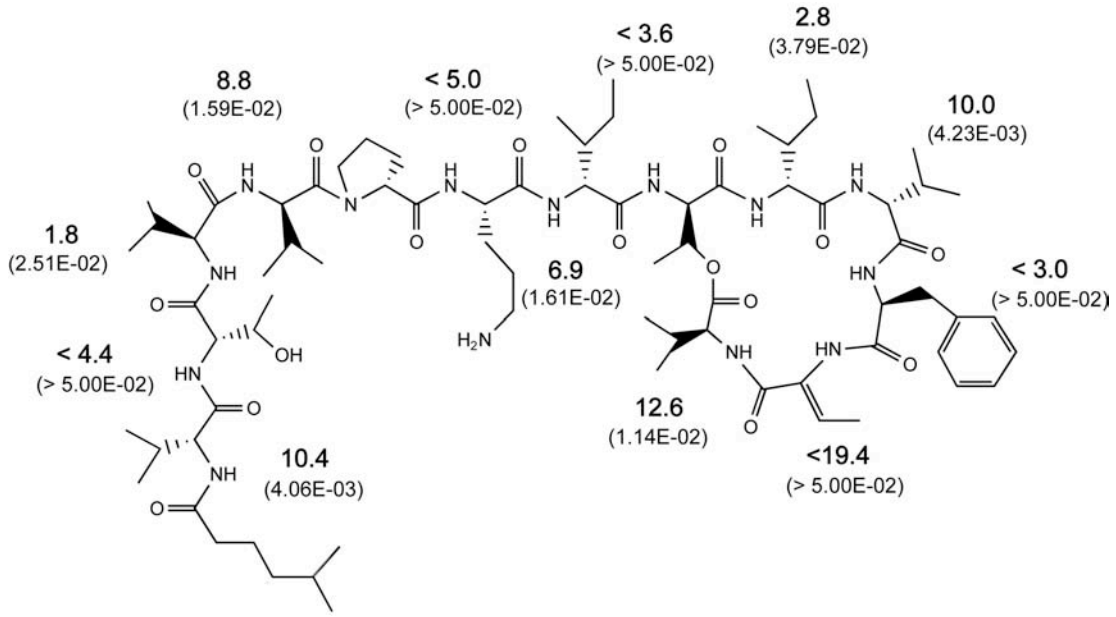

Figure 78: Kahalalide F chemical structure. Protection Factors are plotted for each amide and in brackets their corresponding observed exchange rates (min^{-1}).

After considering the limitations of both PF and K_{obs}, it still seems clear that there are a certain amides remarkably protected from solvent exchange. Amides 2, 14 and 11 are amongst the least exposed; closely followed by 5 and 8, the rest show either low protection factors or exchange too fast to be measured.

Interpretation of this data should take into account that both micelle insertion and hydrogen bonding may lead to similar effects on exchange rate values. Also, it would seem that Temperature Coefficients and protection factor are somewhat complementary when it comes peptide/micelle systems; both shed light on amide hydrogen bonding but only the latter carries information on peptide micelle location. It makes sense then to find agreement between the two parameters for amides 11 and 14 in the C-terminus cycle, meaning that they may be involved in some sort of hydrogen bond, while the other amides in the macrocylce could be more exposed to the solvent.

On the other hand, amides 2 and 5 have high protection factors, while their temperature coefficients wouldn't suggest any hydrogen bonding. This apparent discrepancy between T_{coeff} and PF could imply a preferred inner localization in the SDS micelle for these amides. Similarly, the relatively low PF for amide 8 and its remarkably low T_{coeff} could be explained by a hydrogen bond with a preferred location close to the micelle water interface.

3.3.6 PARAMAGNETIC REAGENTS

Paramagnetic compounds, those with unpaired electrons, are found in a wide variety of applications, from biomembrane characterization by EPR, to contrast agents in Magnetic Resonance Imaging (MRI). However, its usage in solution NMR has been limited due to the deleterious effects of unpaired electrons on nuclear relaxation properties. In recent years this trend has been somehow corrected by incorporating constraints obtained from paramagnetic nuclei into the structure calculation and refinement process; examples of this are a number of metallo-protein studies.[60] Also, taking advantage of their intrinsic magnetic anisotropy, paramagnetic species have been applied to induce partial alignment on proteins, followed by RDC measurement and structure calculation; this property has led to the design of lanthanide-chelating tags as a somewhat general strategy. [61]

Unpaired electrons have the ability to induce broadening on resonances in a distance dependant manner. This is the reason why traditional NMR methods have often failed to characterize paramagnetic proteins and turned instead to X-RAY or EPR for structural insight. Yet this very same effect has been used to qualitatively localize peptide and protein resonances on detergent environments, probably a prelude to the more accurate constraints obtained nowadays from paramagnetic species. [56, 62]

For this purpose, a series of probes such as 5-Doxyl Stearic Acid (DSA) and 16-DSA (Figure 79), typically used in EPR membrane studies, are incorporated in the micelle/water media in order to induce selective broadening to close-by resonances. Both molecules are stearic acid versions with a nitroxide group on different hydrophobic tail carbons. 5-DSA and 16-DSA are incorporated to the detergent media much in the same way as a SDS molecule: hydrophobic moiety embedded within the micelle and the charged acidic function oriented towards water. The difference though, is that while the former induces selective broadening resonances nearby 1-3 SDS carbons, in the micelle's surface surroundings; the latter broadens resonances at the micelle core especially those close to SDS carbons 10-12.[63] The last paramagnetic reagents used in these studies are the water-soluble Toac or Mn2+ salts. They are the DSA negative image and will induce selective broadening on those resonances exposed to the aqueous medium.

Selective broadening effects produced by the above reagents yield a qualitative picture for peptide resonance localization within a micelle; for instance a resonance sitting in the hydrophobic core will be far more affected by 16-DSA than 5-DSA or Mn^{2+} salts; on the contrary, solvent exposed resonances will not suffer much relaxation enhancement in presence of 16-DSA. During the following paragraphs we will illustrate our efforts in trying to build such a model for Kahalalide F location in detergent aggregates.

Broadening on the micelle-embedded peptide is evaluated by comparing 1D 1H and/or 2D- TOCSY with and without each paramagnetic compound; this is done quantitatively using peak intensity or integration for each experiment.

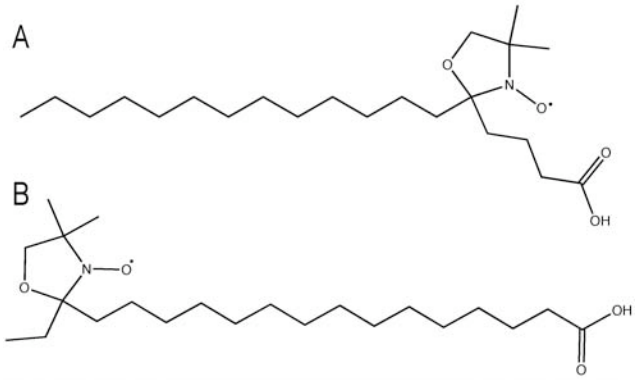

Figure 79: Chemical structure for Doxyl Stearic Acid paramagnetic probes. A) 5-DSA, B) 16-DSA.

3.3.6.1 5-DOXYL STEARIC ACID

For the sake of consistency with the other experiments, KF concentration was kept to 2 mM, and SDS concentration to 50 mM. ^{1}H Watergate and 2D-TOCSY experiments for the free and 5-DSA containing sample were performed at 283K, similar to those used before. Following control experiments, paramagnetic reagent is typically added to a concentration no higher than 1 DSA molecule per SDS micelle particle to avoid excessive broadening of peptide resonances. Again, considering a micelle composed of around 60 to 100 SDS molecules, 0.5 mM 5-DSA seems a reasonable concentration; and according to Figure 80 this is a good compromise between selective broadening and S/N for the observation for most amides.

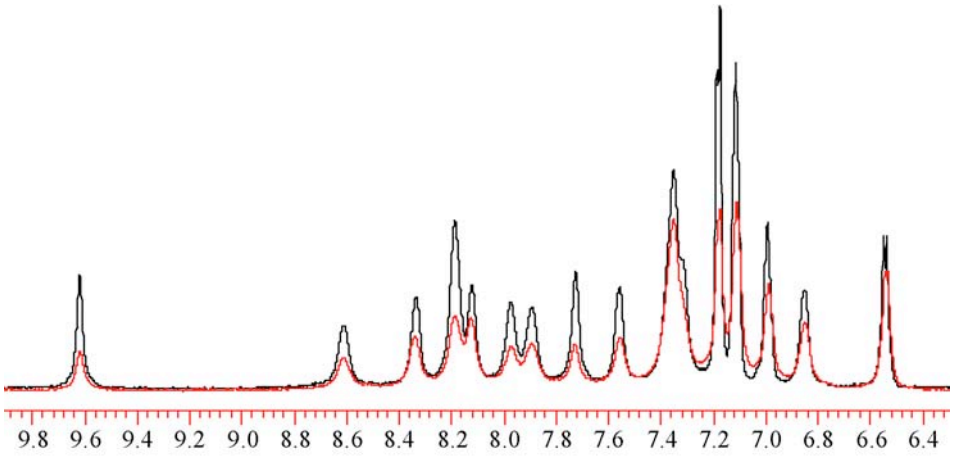

Figure 80: Amide region of a ^{1}H experiment for a 2 mM Kahalalide F sample in water/SDS 50mM. (Black) In the presence of 0.5mM 5-DSA (Red).

Selective broadening effects are analyzed either by peak integration for the 1D spectra or cross peak volume analysis for the 2D-TOCSY spectra (Figure 81). Both methods are often applied to amide protons, and have similar success when no overlap issues exist. However, the use of the 2D-TOCSY peptide fingerprint region is useful not only to circumvent resonance overlap but also to extract information regarding selective broadening on Hα and Hβ protons.

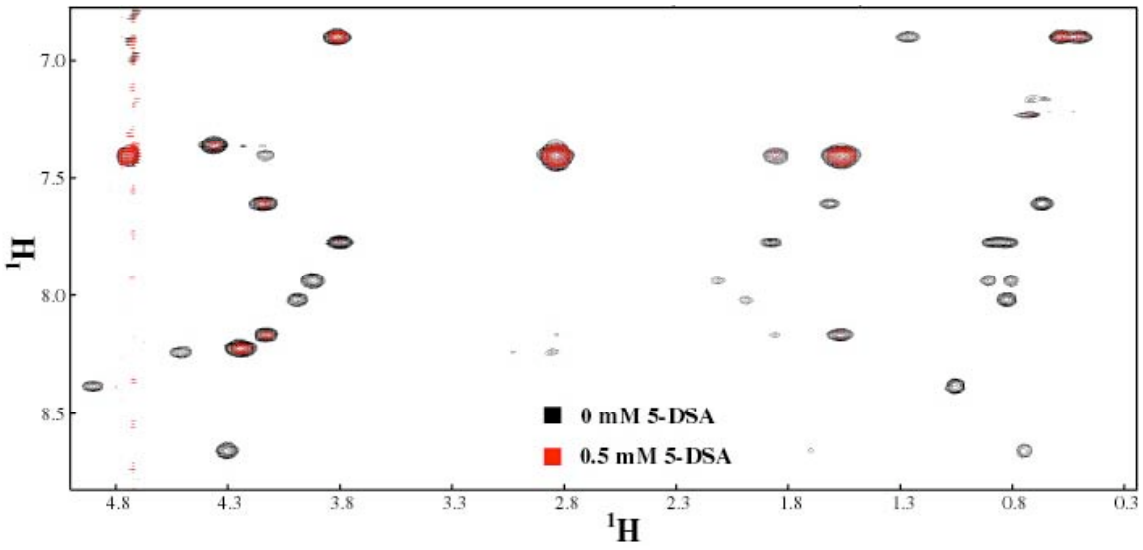

Figure 81: Overlaid 2D-TOCSY fingerprint regions for samples: (Black) 2mM Kahalalide F in water/SDS 50 mM, (Red) plus 0.5 mM 5-DSA.

3.3.6.2 16-DOXYL STEARIC ACID

As in the previous section, a 2 Mm KF 50 mM SDS sample was prepared and the same NMR experiments performed. In contrast to 5-DSA, 100:1 (SDS:DSA) ratio proved too high; since at 0.5 mM 16-DSA a number of amide resonances were broadened beyond detection, a fact that would eventually complicate structural interpretation. This fact alone bespeaks of KF's inclination towards the detergent micelles hydrophobic core, where it probably remains most of the time. Thus, we decided to perform the experiments at a lower 16-DSA concentration (0.3 mM), while the analysis proceeded as described in the previous section.

A rough analysis on sequence-dependent resonance broadening for KF seems to yield a similar profile both for 5 and 16-DSA reagents (Figure 82). N-terminus acylated amide is highly affected by DSA probes, and as we move along the peptide sequence broadening decreases slightly until a local maximum is reached, either on residue 3 or 4(depending on the particular probe), followed by a broadening increase on residue 5. Residues 7 through 9 do not seem particularly affected by either paramagnetic compound, but as we move into the macro-lactone, amide signals decrease in their intensity and reach a minimum on Phe12 amide. Residues 13 and 14 seem to recover rather abruptly from the DSA relaxation effects and the latter becomes one of the least affected resonances throughout KF.

Beyond the similarities in their broadening preferences 5-DSA and 16-DSA differ on their behavior; to start with, different concentrations of each probe have been used due to the greater effects displayed by 16-DSA. Moreover several residues, according to the normalized plot (Figure 82), seem more affected by the deepest probe (16-DSA) than they are by 5-DSA. These residues are mainly located at the hydrophobic N-terminus 1 through 5, and also in part of the c-terminus macro cycle: 10,11,12 amino acids.

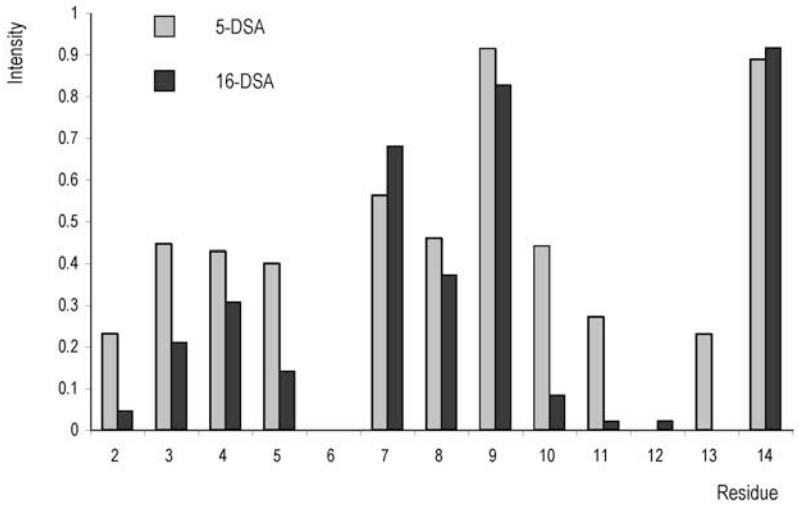

Figure 82: Normalized residual intensity for KF amides upon addition of DSA paramagnetic probe; (Gray) 5-DSA, and (Black) 16-DSA. Hα-HN 2D-TOCSY cross peak intensity was used for all amino acids, except 9 and 13 for which Hβ-HN and $HN_{diagonal}$ peaks were used respectively.

Plotting this information on the peptide sequence reveals an interesting pattern: the central part of the peptide remains relatively unaffected (grey area Figure 83) by either probe. This region is flanked by residues whose amides are particularly broadened by 16-DSA, which places its radical at the very core of the SDS micelle.

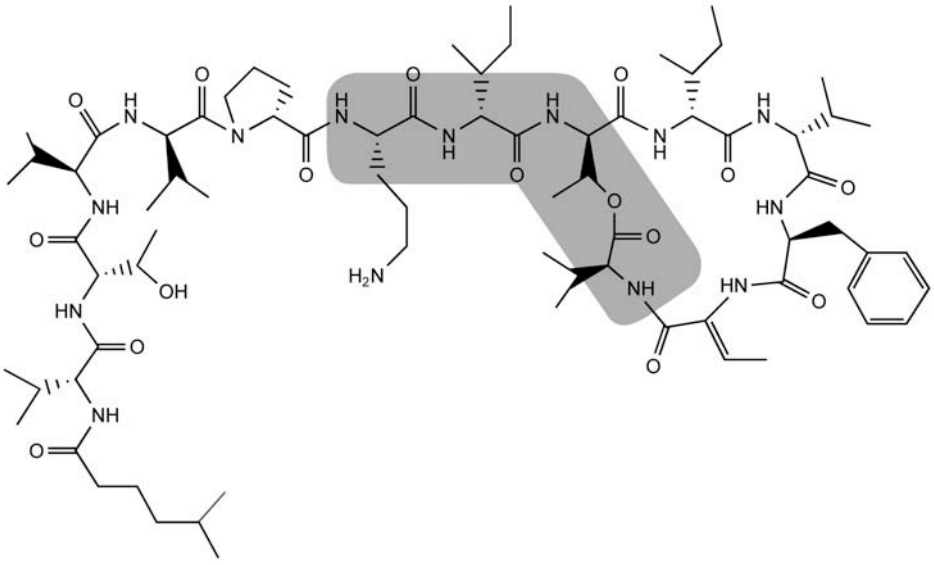

Figure 83: Kahalalide F chemical structure, shaded residues are those whose amides are the least affected by the presence of either 5 or 16-DSA.

As already mentioned, this data can be interpreted in terms of relative position in the micelle, hence the segments of the peptide spending more time within the micelles core will be more affected by the doxyl in

16-DSA than in 5-DSA; these are the non-shaded residues in Figure 83. The central (shaded) part remains nearly unaffected by either DSA compounds and it is only for amide 7 that we observe a slightly larger broadening with 5-DSA than 16-DSA. Not surprisingly, and as already anticipated, this agrees with this part being located close to the micelle/water interface in such a way that ornithine's side-chain can be solvent exposed and interact with SDS charged polar heads simultaneously.

Another interesting feature is the broadening pattern observed from amides 2 through 5 with a signal maximum around residue 3. This effect may be driven by the presence of threonine's side chain, and although the methyl hexanoic moiety anchors the N-terminus tail to the inner part of the micelle, Thr's hydroxyl may be "pulling" part of the tail towards the polar micelle surface.

3.3.7 2D-NOESY AND STRUCTURAL CALCULATION

Throughout the previous sections we have gathered evidences of conformational preference for Kahalalide F in SDS micelles. However, most of them can only be interpreted qualitatively and, with the single exception of hydrogen bonding, would be difficultly implemented into a structure determination protocols. Structure calculation using experimental NMR constraints has traditionally relied on nOe measurements, even more so for unlabeled peptides. These are often introduced into simulated annealing protocols as quantitative or semi-quantitative distance constraints, in the form of an extra potential energy term that has to be minimized along with rest of energy arising from the molecular geometry.[64]

But in order to use nOe restraints properly one has to make sure that the relationship between nOe intensity and inter-proton distance follows an r^{-6} relationship, since under some circumstances spin diffusion, or the presence of multiple proton-proton cross-relaxation pathways may introduce artifacts on the calibration of eventual nOe restraints.[65] This can be diagnosed by performing what is called a NOESY build up curve: a series of experiments with increasing mixing times are recorded, and the occurrence of spin diffusion is readily detected when the plot nOe intensity versus mixing time is no longer linear.

3.3.7.1 NOESY EXPERIMENTS

NOESY experiments with different mixing times (T_{mix}= 100, 200, 300, 400 and 500 ms) were performed for the 6 mM KF in a water/150 mM SDS sample. A small set of cross-peaks from each experiment was used to obtain the NOESY build up curve.

Build-up plots show clear spin diffusion effects beyond 300 ms mixing. (Figure 84) Conversely 200 ms NOESY experiment seems to be a good compromise between nOe intensity and spin diffusion artifacts, which will allow us to obtain the maximum number of reliable distance constraints. On the other hand, mixing time figures agree with the large correlation time one would expect from a protein like molecule; and as already mentioned is a strong evidence for KF-SDS micelle interaction.

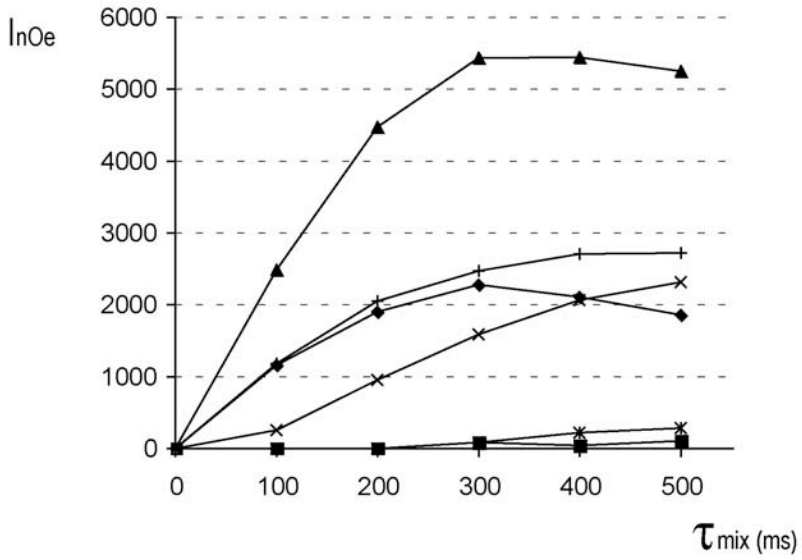

Figure 84: NOESY build-up curves for 6mM Kahalalide F in a water/SDS 150mM sample: Intensity of several arbitrary nOes throughout the series of experiments have been plotted versus the particular T_{mix} used.

3.3.7.2 XPLOR SIMULATED ANNEALING CALCULATION

Once the 200 ms NOESY experiment had been selected, nOe correlations were identified using the aforementioned assignment, integrated and classified according to their intensity: strong, medium, weak and very weak. Distance calibration was performed semi-quantitatively assigning an upper limit distance to every cross-peak in each class: 2.7 Å for strong nOes, 3.4 Å medium, 4.5 Å weak and 6 Å to very weak.

In the end, 79 (33 sequential and 46 non-sequential) distance restraints were introduced into XPLOR [66] standard simulated annealing protocol. Using a modified Charmm19 force field to account for Kahalalide F peculiarities 50 structures were produced, from which the energetically 10 best were finally selected as the solution ensemble (Figure 85).

Energy statistics for the structure ensemble are presented in Table 5. There, we can see none of the selected structures violates any distance constraint, and that the overall molecular geometry for the ensemble does not have an important energy overhead.

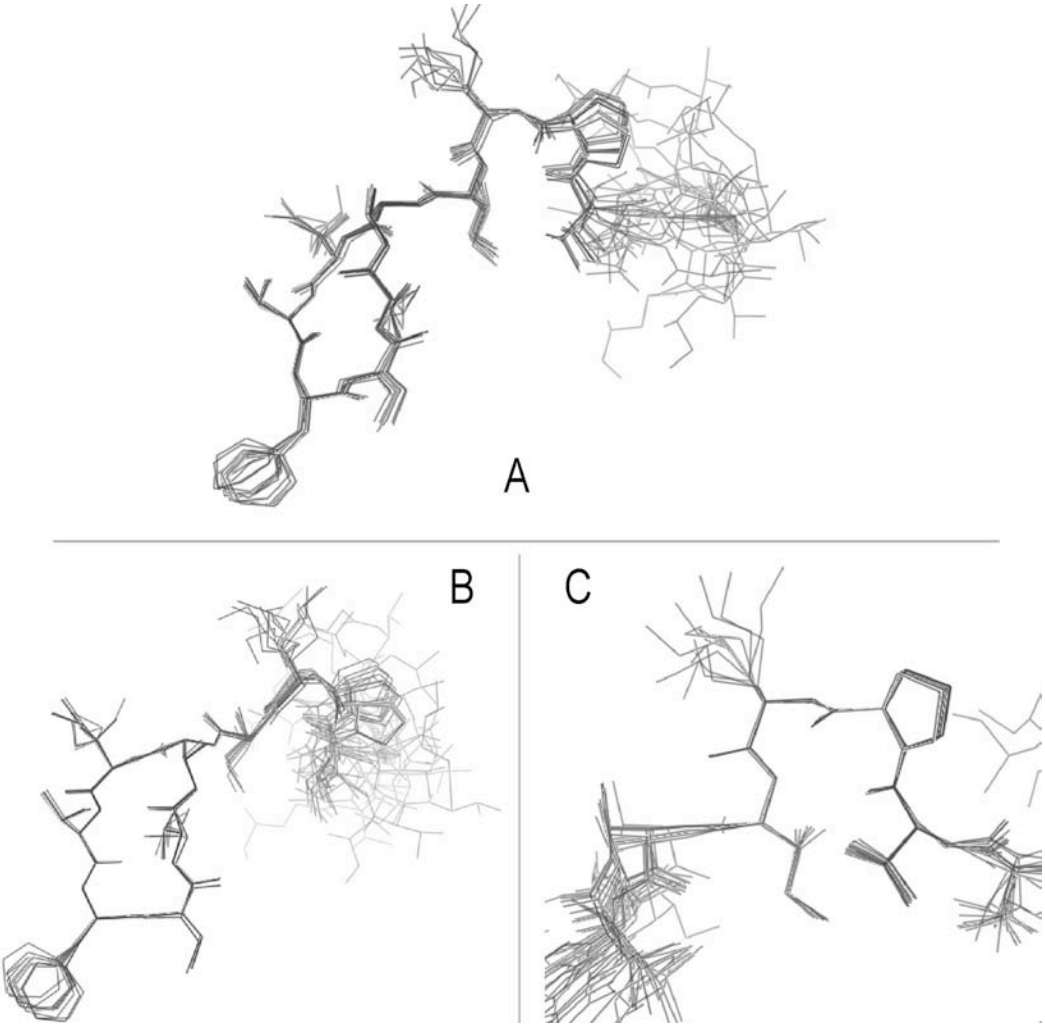

Figure 85 Ensemble of the 10 best structures produced by the simulated annealing protocol. A) Structures have been superimposed from: A)residues 5 through 14; B) residues 9-14; and C) From residue 5 through 8.

Overlap of all selected structures yields a fairly good RMSD of 1.5 Å for backbone atoms. But interestingly if one performs a pairwise alignment of all structures for residues 5 through 14 the RMSD (Figure 85, Table 5) improves remarkably to 0.34 Å. This is the result of a largely unstructured N-termini section (1-5) lacking in medium and long distance nOes, mainly dominated by sequential contacts.

A similar segmental alignment reveals two extraordinarily stiff structural motifs; these are 5 through 8 residue turn and C-terminus cycle with backbone RMSD values of 0.13 Å and 0.09 Å respectively. It is also interesting to note that for the region encompassing both motifs (residues: 5-14) overlaps considerably worse –with a 0.34 Å backbone RMSD- than the individual substructures, suggesting certain ambiguity in the relative orientation between cycle and turn (Figure 85). For this reason it seems safe to analyze each structural motif separately throughout the following sections.

Energy (kcal/mol)	Total Energy	45.26	±1.14		
	Bond energy	1.54	±0.18		
	Angle energy	23.89	±0.31		
	Out of plane energy	2.97	±0.14		
	Non-bonded energy	10.77	±0.87		
	nOes	6.09	±1.16		
	dihedral	---	---		
nOe statistics	total	79			
	sequential	33			
	non-sequential	46			
	nOe violations >0.2 (Å)	0			
	Average violation (Å)	±0.039			
		Backbone atoms (Å)		Heavy atoms (Å)	
RMSD	KF (0-14)	1.50	±0.43	2.41	±0.61
	KF (5-14)	0.34	±0.14	2.81	±0.69
	KF (5-8)	0.13	±0.07	2.89	±0.65
	KF (8-14)	0.09	±0.05	3.11	±0.80

Table 5: Energy, nOe and RMSD statistics for the structure ensemble produced by simulated annealing protocol.

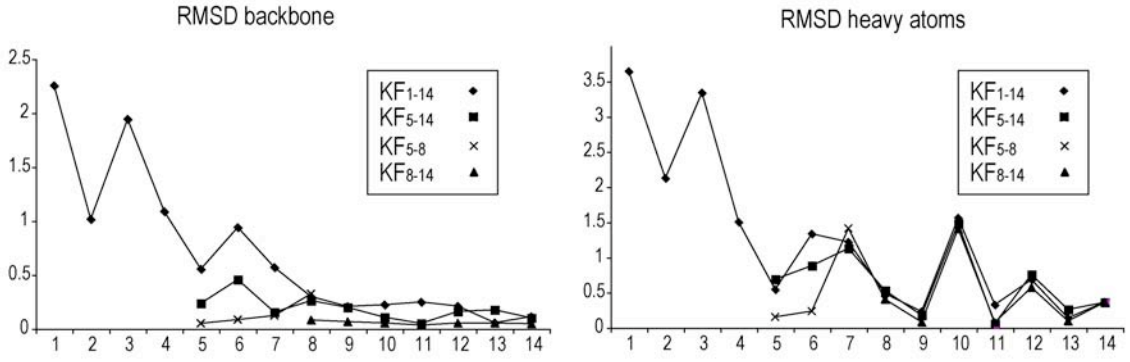

Figure 86: RMSD values for the lowest energy structure with respect to the ensemble average computed for each amino acid's backbone (left) and heavy atoms (right). RMSD calculations have been repeated using different Kahalalide F stretches: whole sequence, 5-14, 5-8, and C-terminus cycle residues: 8 through14.

3.3.7.3 C-TERMINUS

19 membered C-terminus macro cycle shows a typical two trans annular hydrogen-bond motif often encountered in cyclic peptides [52]; which together with Z-DhB's limited conformational space contribute to an overall flat anatomy for the macrolactone. As a result, side chains of facing valines 10 and 14 sit on opposite sides of the plane defined by the hydrogen bonds. (Figure 87)

β-turn induction has traditionally attracted much interest, and a number of groups have engineered non-proteinogenic amino acids that once introduced in a peptide sequence stabilize the otherwise unpopulated β-turn ψ φ region.[67] Among the most frequently encountered β-turn inducers are α–β dehydroamino acids, they are fairly "non-invasive" and are even found within many natural products. Both theoretical and experimental works[68, 69] suggest that such amino acids are able to induce a various types ofβ turns in peptide sequences; in particular α–β dehydroamino acids located at i+1 tend to favor βII', whereas at i+2 they usually stabilize βII turns.

Indeed, the analysis of 12-13 turn reveals φ and ψ angle values (Figure 87) for these residues close to the ideal βII turn values (-60, 120, 80, 0 for φi+1, ψi+1, φi+2, ψi+2 respectively). This observation is not surprising given the presence of various diagnostic nOes for a type II turn in this part of KF (Figure 87): strong $H\alpha_{i+1}$-HN_{i+3} (between 12-14) and strong HN_{i+3}-HN_{i+4}. (13-14). Furthermore, nOe contacts across the macrolactone such as 10HN-11HN and 10Hα-14HN seem to contribute to the observed hydrogen bond pattern as well as to turn formation in the simulated annealing. (Figure 87) Interestingly, the hydrogen bond pattern is also corroborated by some evidences not included in the structure calculation –namely temperature coefficients and amide exchange rates or protection factors-. Both parameters seem to agree that amides 10 and 14 are particularly protected from solvent.

With regard to the turn centered at the C-terminus depsipeptide bond, this seems to be experimentally supported by the presence of strong nOes between 10HN-11HN and 9Hβ-11HN. Which produce a pseudo βII turn formed by Val14, allThr9, alloIle10 and Vall11 as i, i+1, i+2 and i+3 respectively; and stabilized by a pseudo (i→ i+3) hydrogen bond and nOes which would typically correspond to (HN_{i+3}-HN_{i+4}) and ($H\alpha_{i+1}$-HN_{i+3}) in βII turns. Similar pseudo-β turns, with a C11 geometry in the hydrogen bond pattern, have been mentioned in the past in the context of β-peptides and foldamers, particularly in cyclic oligomers that intercalate α and β amino acids. [70] [71]

Interestingly, in our structure the ester dihedral angle is not planar; a fact that probably relieves certain tension in this pseudo-β turn and allows de formation of the pseudo (i→ i+3) hydrogen bond. Indeed, one could argue this is the reason why a depsipeptidic linkage is used to close the macrocycle rather than its isoster amide.

Another remarkable feature in this pseudo-β turn is the orientation of alloIle10 amide; which in our structure ensemble tends to be oriented towards Val14 carbonyl, probably forming a distorted hydrogen bond that presents a C7 geometry comparable to a γ-turn. Such distortion could probably explain its apparently contradictory temperature coefficient and amide exchange values.

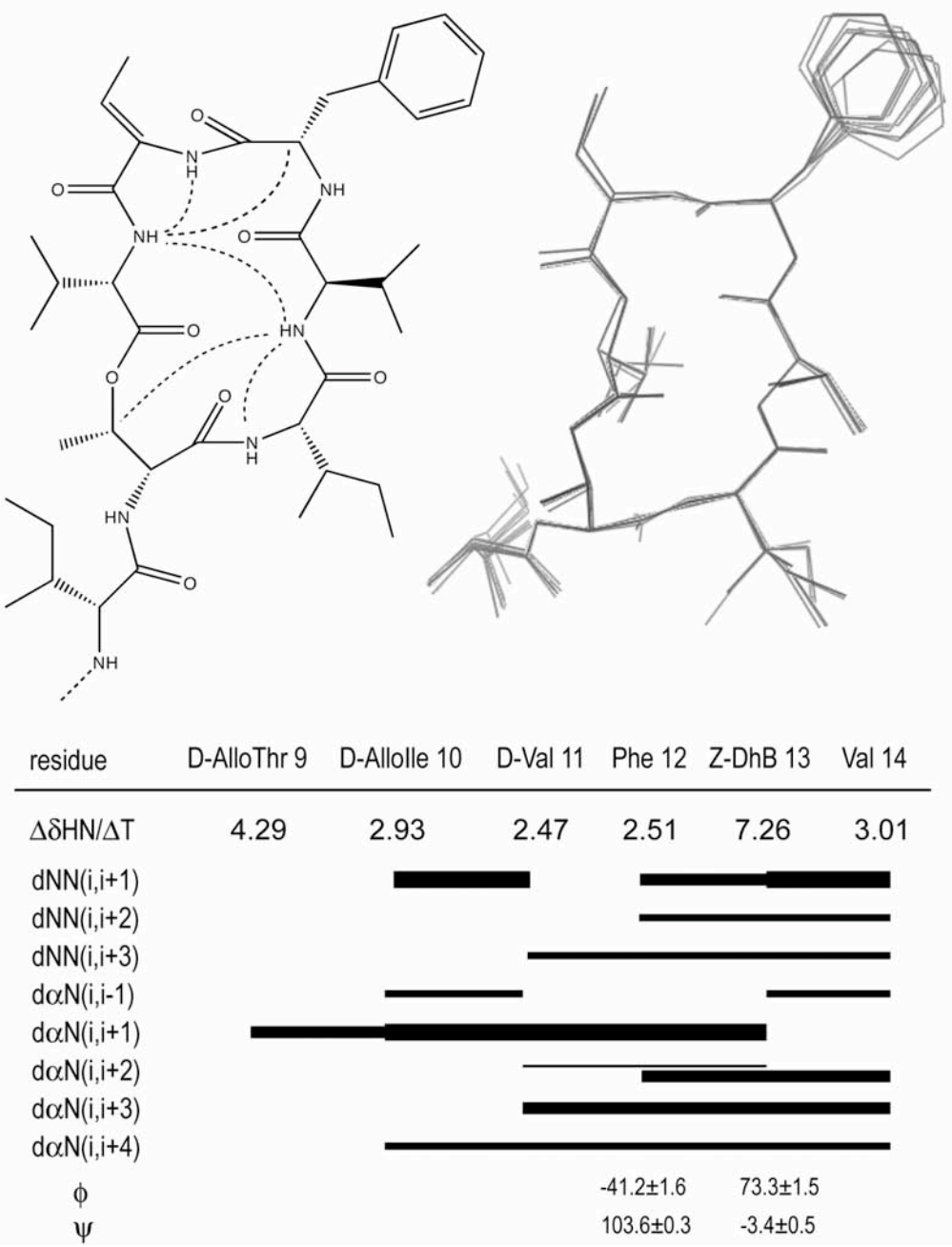

Figure 87: Kahalalide F (residues 8 through 14) chemical formula and ensemble of 10 energetically best structures generated by SA protocol. Figure includes relevant NMR information: temperature coefficients (ppb/K), nOe contacts presented as lines with varying thickness according to their intensity. Φ and Ψ angles for relevant turn amino acids are also shown.

3.3.7.4 5-8 TURN

According to RMSD values the other highly structured region in KF is the tight turn composed by D-Val5, D-Pro6, L-Orn7 and D-AlloIle8. From the angle values we can say that this adjusts to a canonical type II turn,

and indeed typical nOes for this motif are readily identified (Figure 88). Temperature coefficients and amide exchange rates also support the presence of and hydrogen bond where D-allolle8 is involved.

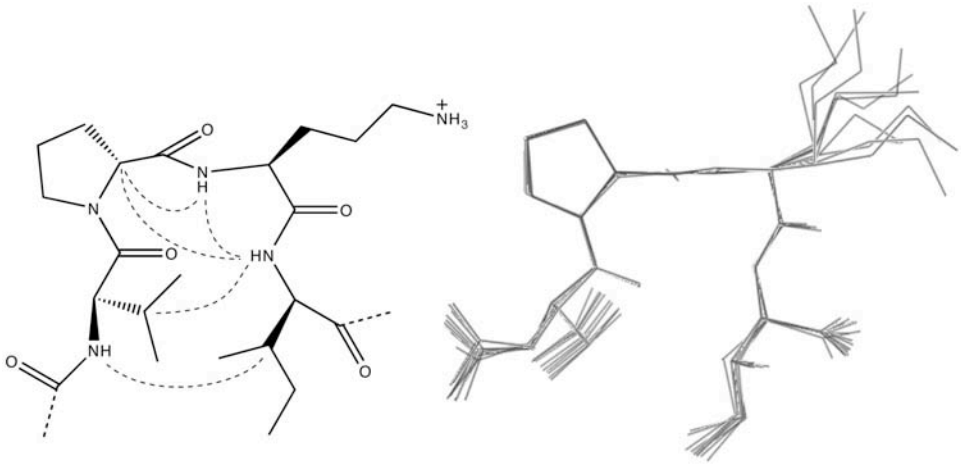

residue	D-Val 5	D-Pro 6	L-Orn 7	D-allolle 8
ΔδHN/ΔT	6.33	—	6.71	0.78
dNN(i,i+1)				
dNN(i,i+2)				
dαN(i,i-1)				
dαN(i,i+1)				
dαN(i,i+2)				
dβN(i,i-3)				
dβN(i,i+3)				
ϕ		56.7±0.4	-71.6±8.6	
ψ		-134.0±0.5	-17.5±9.8	

Figure 88: Kahalalide F (residues 5 through 8) chemical formula and ensemble of 10 energetically best structures generated by SA. Includes relevant NMR information: temperature coefficients (ppb/K), nOe contacts presented as lines with varying thickness according to their intensity. Φ and Ψ angles for relevant turn amino acids are also shown.

D-amino acid substitution in otherwise all-L-sequences has been extensively applied to induce β-turn motifs, as described by Gellman et al in a number of publications.[72-74] Most often these include D-proline at i+1 position of a β-turn type II', usually followed by a glycine; but β-turn propensity has also been described for peptides with Pro-D-Xaa as the nucleating sequence. [75] The latter situation is similar to ours, except for the reversed chirality, since our turn sequence is all-D with the exception of ornithine at i+2. Trans D-Pro6 has an important role in the bend but without the "reversed" Orn, i+1 and i+2 side chains would unavoidably clash and the type II turn would be as improbable as it is in all-L sequences. The same argument could be applied to justify the particular D/L configuration for the rest of amino acids in this turn, and may explain the biological inactivity of Rinehart's alleged Kahalalide F, where Val 4 and Val 5 have their chiralities swapped. [19]

Biological relevance of this turn is currently being addressed in our laboratory, and Kahalalide F analogues containing 5-8 cross-linked side-chains have been designed and synthesized to stabilize the turn motif. Preliminary biological assays for some of these analogues seem to indicate that their antitumoral activity is not lost, this is an encouraging observation given the long record of failed analogues with similarly significant chemical modifications. All in all, this suggests a relationship between the peptide's ability to form this turn and its biological activity.

3.3.7.5 LINKER

Individual 5-8 β-turn and 9-14 C-terminus macro-cycle motifs have a very low RMSD, however if we consider the segment running from residue 5 through 14 its RMSD is considerably higher. (See Figure 85(A),Figure 86 and Table 5). This observation is probably due to the poor definition for the cycle-turn linker in our structure ensemble. A deeper analysis however, reveals that this is caused by the lack of nOes for residue 8; which could either be a result of an intrinsically flexible linker, a result of the severe overlap between residue 7 and 8 that hampers reliable nOe assignment or a combination of both.

3.3.7.6 N-TERMINUS

With regard to the N-terminus section –residues 1 through 5 residues- it is clear from its RMSD values (Figure 86) that it is largely unstructured and flexible. In most structures nonetheless, a bent can be observed around Thr3 that is a consequence of some weak non-sequential nOes between Val4 amide and the Hα protons in the methyl-hexanoic acyl group. Additionally, some weak nOes established between Val2 amide and Val4 amide and Hα may explain this bending propensity, although they are not enough to produce a more rigid structure in this part of Kahalalide F.

3.3.8 STRUCTURAL MODEL FOR KF MEMBRANE INTERACTION

So, after carefully harvesting structural information for Kahalalide F from various experiments and across different media it seems appropriate to try and build a model for the interaction of Kahalalide F with biological membranes,

Raw structural information, both qualitative (T_{coef}, k_{obs}/PF) and quantitative (nOe's and SA-derived ensemble), agree on the structural preferences for the peptide in membrane-like environments. In a micellar environment this structure can be dissected in three differentiated parts, as guided by pairwise RMSD: C-terminus macro cycle, 5-8 turn, and N-termini tetra peptide. The first two are quite rigid, at least when analyzed separately, not so when it comes to their relative orientation and are stabilized by a network of hydrogen bonds coherent with all our experimental data: nOe based SA calculation and qualitative data (T_{coef}, PF). With regard to the latter part, this is largely unstructured, albeit it has some preference towards a bent conformer.

The scenario is structurally much simpler both in water and DMSO, in both cases we can only distinguish two segments: C-terminus macro cycle, and an exo-cycle N-terminus tail. The C-terminus as in the case of SDS micelles is rigid, and although a thorough calculation has not been carried out, all data ($^3J_{\alpha N}$ and T_{coef}) suggest a similar structure to that in SDS/water micelles, held by the same hydrogen bond network. In the particular case of DMSO (T_{coef} information readily reveals which are the exposed and hydrogen bonded amides, even more distinctly than in SDS/water. As for the N-terminus tail, it is unstructured and intrinsically

flexible in both conditions; albeit there are also some evidences implying it is not completely random coil and that there might be some turn preference within.

Simulated annealing calculations using SDS/water NMR data were carried out in vacuum; as a result, with this information is not possible to determine how the peptide is inserted or its relative orientation in the detergent micelle. Nonetheless, evidences such as line width and chemical shift differences observed upon SDS/water solubilization clearly indicate a high degree of insertion in SDS particles.

In order to obtain a insight on the peptide/micelle insertion one has to turn to using paramagnetic probes. The result of these experiments was not completely unforeseen and in general confirms our intuition, which anticipated the location of the central ornithine close to the water/micelle interface to maximize water exposure and charge complementarity. The same rational applies to threonine's hydroxyl that despite its aliphatic neighbors also tries to maximize water exposure and is probably responsible for the turn preference observed on the N-terminus segment. As for the apolar "ends" of the molecule (methylhexanoic moiety and Z-Dhb-Phe turn) these tend to be deeply buried in the micelle's hydrophobic core. The static picture for peptide/micelle complex provided by these results is however only qualitative; since this is indeed a very dynamic system, and as the results of such experiments provide time-averaged information that has to be considered with caution. With this in mind it is still possible to use the above data to build an tentative model for the monomeric insertion of KF into SDS micelles Figure 89.

The model presented in Figure 89 seems quite reasonable. All the hydrophobic parts of the molecule are located well into the hypothetical sphere defined by SDS, while most hydrophilic sections of the molecule have been placed towards the charged SDS sulphate surface. Reassuringly, molecule structures produced by the SA protocol show some sort of curvature along the sequence and, when these are placed within a model micelle, peptide curvature resembles that of SDS micelle surface.

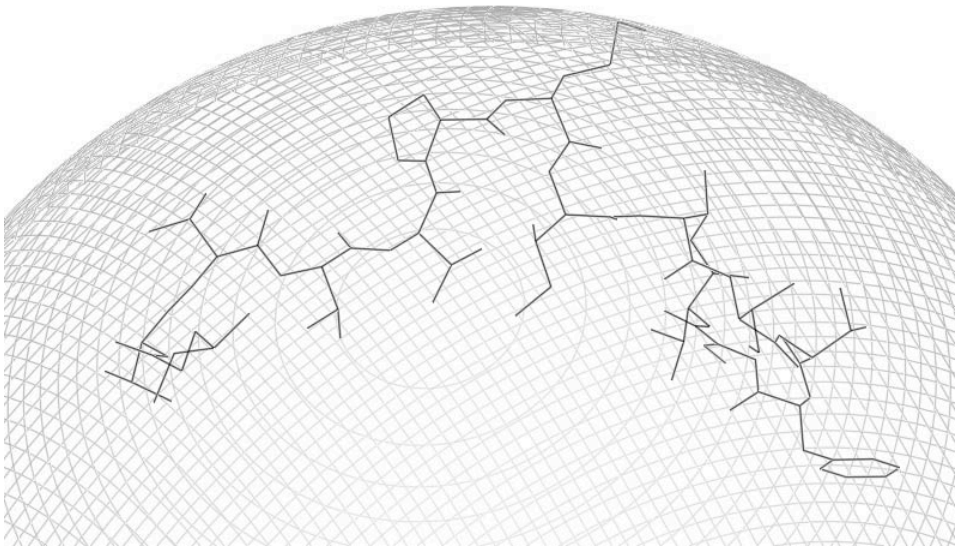

Figure 89: Model presenting Kahalalide F within an SDS micelle. Kahalalide F structure corresponds to best structure generated by the SA protocol and has been manually positioned within a micelle model to agree with DSA broadening data. Meshed surface corresponds to detergent micelle model, calculated using SDS molecular length as radius.

All in all it is clear that Kahalalide F preferentially inserts in lipid environments, and there tends to adopt a remarkably folded conformation. Also, given that Kahalalide F cytotoxic effects seem to occur primarily at a membrane level, this folded state could be very relevant to explain its antitumoral activity. It is possible that interaction with the membrane and preorganization into our proposed structure are necessary for the peptide to interact with its membrane receptor. Such receptor has not yet been identified; nonetheless interaction between Kahalalide F active state and this hypothetical receptor would activate the cellular signaling pathways that ultimately induce cellular death. In such mode of action, Kahalalide would act individually on its protein target and knowledge of the active conformation could be used to design novel analogs with improved activity, toxicity or bioavailability profiles; as it is often done in medicinal chemistry programs.

On the other hand, the presented model does not rule out a much more basic mode of action. This mechanism would consist on the peptide inserting into the membrane, either individually or organized into some sort of aggregate, and then destabilizing the cellular membrane through pore formation or some other mechanism; and as it happens with some antibiotic peptides, membrane leakage would occur and cells would eventually die. Some of the presented data suggests that indeed KF has the ability to assemble into aggregates, thus a mechanism where multiple copies of the peptide, rather than a single molecule of KF, exert the cytotoxic effect is very plausible. Unfortunately, our structural study has been carried out under conditions where Kahalalide F is isolated in the lipid environment; for this reason, should the latter mechanism be true, our proposed active conformation might be inaccurate and as a result we would not be able to establish a reliable structure activity relationship. For these reasons, such putative oligomerization mechanism should in the future be explored, probably combining techniques such as ssNMR and TEM.

3.4 BIBLIOGRAPHY

1. Cragg, G.M., D.J. Newman, and S.S. Yang, *Natural product extracts of plant and marine origin having antileukemia potential. The NCI experience.* Journal Of Natural Products, 2006. **69**(3): p. 488-498.
2. Newman, D.J. and G.M. Cragg, *Marine natural products and related compounds in clinical and advanced preclinical trials.* J Nat Prod, 2004. **67**(8): p. 1216-38.
3. Simmons, T.L., et al., *Marine natural products as anticancer drugs.* Mol Cancer Ther, 2005. **4**(2): p. 333-42.
4. Tincu, J.A. and S.W. Taylor, *Antimicrobial peptides from marine invertebrates.* Antimicrob Agents Chemother, 2004. **48**(10): p. 3645-54.
5. Costantino, V., et al., *Chemical diversity of bioactive marine natural products: an illustrative case study.* Curr Med Chem, 2004. **11**(13): p. 1671-92.
6. Zhang, L., et al., *Exploring novel bioactive compounds from marine microbes.* Curr Opin Microbiol, 2005. **8**(3): p. 276-81.
7. Donia, M. and M.T. Hamann, *Marine natural products and their potential applications as anti-infective agents.* Lancet Infect Dis, 2003. **3**(6): p. 338-48.
8. Blunt, J.W., et al., *Marine natural products.* Nat Prod Rep, 2005. **22**(1): p. 15-61.
9. Konig, G.M., et al., *Natural Products from Marine Organisms and Their Associated Microbes.* Chembiochem, 2005.
10. Rinehart, K.L., et al., *Structures Of The Didemnins, Anti-Viral And Cyto-Toxic Depsipeptides From A Caribbean Tunicate.* Journal Of The American Chemical Society, 1981. **103**(7): p. 1857-1859.
11. Rinehart, K.L., *Antitumor compounds from tunicates.* Medicinal Research Reviews, 2000. **20**(1): p. 1-27.
12. Jou, G., et al., *Total synthesis of dehydrodidemnin B. Use of uronium and phosphonium salt coupling reagents in peptide synthesis in solution.* Journal Of Organic Chemistry, 1997. **62**(2): p. 354-366.
13. Sarabia, F., et al., *Chemistry and biology of cyclic depsipeptides of medicinal and biological interest.* Curr Med Chem, 2004. **11**(10): p. 1309-32.
14. Hamann, M.T., et al., *Kahalalides: Bioactive Peptides from a Marine Mollusk Elysia rufescens and Its Algal Diet Bryopsis sp.(1).* J Org Chem, 1996. **61**(19): p. 6594-6600.
15. Hamman, M.T., et al., *Kahalalides: Bioactive Peptides from a Marine Mollusk Elysia rufescens and Its Algal Diet Bryopsis.* J. Org. Chem., 1998. **63**(14): p. 4856-4856.
16. Goetz, G., Y. Nakao, and P.J. Scheuer, *Two Acyclic Kahalalides from the Sacoglossan Mollusk Elysia rufescens.* J. Nat. Prod., 1997. **60**(6): p. 562-567.
17. Garcia-Rocha, M., P. Bonay, and J. Avila, *The antitumoral compound Kahalalide F acts on cell lysosomes.* Cancer Lett, 1996. **99**(1): p. 43-50.
18. Hamann, M.T. and P.J. Scheuer, *Kahalalide-F - A Bioactive Depsipeptide From The Sacoglossan Mollusk Elysia-Rufescens And The Green-Alga Bryopsis Sp.* Journal Of The American Chemical Society, 1993. **115**(13): p. 5825-5826.
19. Bonnard, I., I. Manzanares, and K.L. Rinehart, *Stereochemistry of kahalalide F.* J Nat Prod, 2003. **66**(11): p. 1466-70.
20. Lopez-Macia, A., et al., *Synthesis and structure determination of kahalalide F (1,2).* J Am Chem Soc, 2001. **123**(46): p. 11398-401.
21. Suarez, Y., et al., *Kahalalide F, a new marine-derived compound, induces oncosis in human prostate and breast cancer cells.* Mol Cancer Ther, 2003. **2**(9): p. 863-72.
22. Janmaat, M.L., et al., *Kahalalide F induces necrosis-like cell death that involves depletion of ErbB3 and inhibition of Akt signaling.* Mol Pharmacol, 2005. **68**(2): p. 502-10.
23. Sewell, J.M., et al., *The mechanism of action of Kahalalide F: variable cell permeability in human hepatoma cell lines.* Eur J Cancer, 2005. **41**(11): p. 1637-44.

24. Zasloff, M., *Antimicrobial peptides of multicellular organisms.* Nature, 2002. **415**(6870): p. 389-95.
25. Vila-Perello, M., et al., *Structural dissection of a highly knotted peptide reveals minimal motif with antimicrobial activity.* J Biol Chem, 2005. **280**(2): p. 1661-8.
26. Wagner, G., A. Kumar, and K. Wuthrich, *Systematic application of two-dimensional 1H nuclear-magnetic-resonance techniques for studies of proteins. 2. Combined use of correlated spectroscopy and nuclear Overhauser spectroscopy for sequential assignments of backbone resonances and elucidation of polypeptide secondary structures.* Eur J Biochem, 1981. **114**(2): p. 375-84.
27. Case, D.A., H.J. Dyson, and P.E. Wright, *Use of chemical shifts and coupling constants in nuclear magnetic resonance structural studies on peptides and proteins.* Methods Enzymol, 1994. **239**: p. 392-416.
28. Jao, S.C., et al., *Trifluoroacetic acid pretreatment reproducibly disaggregates the amyloid beta-peptide.* Amyloid-International Journal Of Experimental And Clinical Investigation, 1997. **4**(4): p. 240.
29. Buck, M., *Trifluoroethanol and colleagues: cosolvents come of age. Recent studies with peptides and proteins.* Quarterly Reviews Of Biophysics, 1998. **31**(3): p. 297-355.
30. Kemmink, J. and T.E. Creighton, *Effects Of Trifluoroethanol On The Conformations Of Peptides Representing The Entire Sequence Of Bovine Pancreatic Trypsin-Inhibitor.* Biochemistry, 1995. **34**(39): p. 12630-12635.
31. Searle, M.S., et al., *Native-like beta-hairpin structure in an isolated fragment from ferredoxin: NMR and CD studies of solvent effects on the N-terminal 20 residues.* Protein Engineering, 1996. **9**(7): p. 559-565.
32. Srisailam, S., et al., *Amyloid-like fibril formation in an all beta-barrel protein. Partially structured intermediate state(s) is a precursor for fibril formation.* J Biol Chem, 2003. **278**(20): p. 17701-9.
33. Ohnishi, S., A. Koide, and S. Koide, *Solution conformation and amyloid-like fibril formation of a polar peptide derived from a beta-hairpin in the OspA single-layer beta-sheet.* J Mol Biol, 2000. **301**(2): p. 477-89.
34. Gonzalez, Y.I. and E.W. Kaler, *Cryo-TEM studies of worm-like micellar solutions.* Current Opinion In Colloid & Interface Science, 2005. **10**(5-6): p. 256.
35. Danino, D., A. Bernheim-Groswasser, and Y. Talmon, *Digital cryogenic transmission electron microscopy: an advanced tool for direct imaging of complex fluids.* Colloids And Surfaces A-Physicochemical And Engineering Aspects, 2001. **183**: p. 113.
36. George, S.R., B.F. O'Dowd, and S.R. Lee, *G-protein-coupled receptor oligomerization and its potential for drug discovery.* Nature Reviews Drug Discovery, 2002. **1**(10): p. 808.
37. Walian, P., T.A. Cross, and B.K. Jap, *Structural genomics of membrane proteins.* Genome Biology, 2004. **5**(4).
38. Strandberg, E. and A.S. Ulrich, *NMR methods for studying membrane-active antimicrobial peptides.* Concepts In Magnetic Resonance Part A, 2004. **23A**(2): p. 89.
39. Maslennikov, I.V., E.V. Bocharov, and A.S. Arseniev, *Spatial Structure Of Transmembrane Segment-C, Segment-E, And Segment-G Of Bacterioopsin By 2-Dimensional H-1-Nmr Spectroscopy.* Bioorganicheskaya Khimiya, 1995. **21**(9): p. 659-674.
40. Pashkov, V.S., et al., *Spatial structure of the M2 transmembrane segment of the nicotinic acetylcholine receptor alpha-subunit.* Febs Letters, 1999. **457**(1): p. 117-121.
41. Rastogi, V.K. and M.E. Girvin, *Structural changes linked to proton translocation by subunit c of the ATP synthase.* Nature, 1999. **402**(6759): p. 263-8.
42. Rosevear, P., et al., *Alkyl glycoside detergents: a simpler synthesis and their effects on kinetic and physical properties of cytochrome c oxidase.* Biochemistry, 1980. **19**(17): p. 4108-15.
43. Lauterwein, J., et al., *Physicochemical Studies Of The Protein-Lipid Interactions In Melittin-Containing Micelles.* Biochimica Et Biophysica Acta, 1979. **556**(2): p. 244.
44. Sanders, C.R. and R.S. Prosser, *Bicelles: a model membrane system for all seasons?* Structure, 1998. **6**(10): p. 1227-34.

45. Vold, R.R., R.S. Prosser, and A.J. Deese, *Isotropic solutions of phospholipid bicelles: A new membrane mimetic for high-resolution NMR studies of polypeptides.* Journal Of Biomolecular Nmr, 1997. **9**(3): p. 329.
46. Tjandra, N., et al., *Use of dipolar 1H-15N and 1H-13C couplings in the structure determination of magnetically oriented macromolecules in solution.* Nat Struct Biol, 1997. **4**(9): p. 732-8.
47. Whitehead, T.L., L.M. Jones, and R.P. Hicks, *PFG-NMR investigations of the binding of cationic neuropeptides to anionic and zwitterionic micelles.* Journal Of Biomolecular Structure & Dynamics, 2004. **21**(4): p. 567-576.
48. Whitehead, T.L., L.M. Jones, and R.P. Hicks, *Effects of the incorporation of CHAPS into SDS micelles on neuropeptide-micelle binding: Separation of the role of electrostatic interactions from hydrophobic interactions.* Biopolymers, 2001. **58**(7): p. 593-605.
49. Papo, N. and Y. Shai, *Host defense peptides as new weapons in cancer treatment.* Cellular And Molecular Life Sciences, 2005. **62**(7-8): p. 784.
50. Esposito, C., et al., *Effect of a weak electrolyte on the critical micellar concentration of sodium dodecyl sulfate.* Journal Of Colloid And Interface Science, 1998. **200**(2): p. 310.
51. Opella, S.J., Y. Kim, and P. McDonnell, *Experimental nuclear magnetic resonance studies of membrane proteins.* Methods Enzymol, 1994. **239**: p. 536-60.
52. Kessler, H., *Conformation and Biological Activity of Cyclic Peptides.* Angewandte Chemie International Edition in English, 1982. **21**(7): p. 512-523.
53. Spyracopoulos, L. and J.D.J. Oneil, *Effect Of A Hydrophobic Environment On The Hydrogen-Exchange Kinetics Of Model Amides Determined By H-1-Nmr Spectroscopy.* Journal Of The American Chemical Society, 1994. **116**(4): p. 1395-1402.
54. Woodward, C., N. Carulla, and G. Barany, *Native state hydrogen-exchange analysis of protein folding and protein motional domains*, in *Energetics Of Biological Macromolecules, Pt E*. 2004. p. 379-400.
55. Dempsey, C.E., *Hydrogen exchange in peptides and proteins using NMR-spectroscopy.* Progress In Nuclear Magnetic Resonance Spectroscopy, 2001. **39**(2): p. 135-170.
56. Shao, H., et al., *Solution structures of micelle-bound amyloid beta-(1-40) and beta-(1-42) peptides of Alzheimer's disease.* J Mol Biol, 1999. **285**(2): p. 755-73.
57. Sforca, M.L., et al., *The micelle-bound structure of an antimicrobial peptide derived from the alpha-chain of bovine hemoglobin isolated from the tick Boophilus microplus.* Biochemistry, 2005. **44**(17): p. 6440-51.
58. Bai, Y.W., et al., *Primary Structure Effects On Peptide Group Hydrogen-Exchange.* Proteins-Structure Function And Genetics, 1993. **17**(1): p. 75-86.
59. Wojcik, J., et al., *NMR measurements of proton exchange between solvent and peptides and proteins.* Acta Biochimica Polonica, 1999. **46**(3): p. 651-663.
60. Bertini, I., et al., *NMR spectroscopy of paramagnetic metalloproteins.* Chembiochem, 2005. **6**(9): p. 1536-1549.
61. Nitz, M., et al., *A powerful combinatorial screen to identify high-affinity terbium(III)-binding peptides.* Chembiochem, 2003. **4**(4): p. 272-276.
62. Monticelli, L., et al., *Interaction of bombolitin II with a membrane-mimetic environment: an NMR and molecular dynamics simulation approach.* Biophys Chem, 2002. **101-102**: p. 577-91.
63. vandenHooven, H.W., et al., *Surface location and orientation of the lantibiotic nisin bound to membrane-mimicking micelles of dodecylphosphocholine and of sodium dodecylsulphate.* European Journal Of Biochemistry, 1996. **235**(1-2): p. 394-403.
64. Guntert, P., *Structure calculation of biological macromolecules from NMR data.* Quarterly Reviews Of Biophysics, 1998. **31**(2): p. 145-237.
65. Kumar, A., R.R. Ernst, and K. Wuthrich, *A Two-Dimensional Nuclear Overhauser Enhancement (2d Noe) Experiment For The Elucidation Of Complete Proton-Proton Cross-Relaxation Networks In Biological Macromolecules.* Biochemical And Biophysical Research Communications, 1980. **95**(1): p. 1-6.

66. Brunger, A.T., *XPLOR Manual Version 3.1.* Yale Univ. Press, 1993.
67. Schneider, J.P. and J.W. Kelly, *Templates That Induce Alpha-Helical, Beta-Sheet, And Loop Conformations.* Chemical Reviews, 1995. **95**(6): p. 2169-2187.
68. Thormann, M. and H.J. Hofmann, *Conformational properties of peptides containing dehydro amino acids.* Journal Of Molecular Structure-Theochem, 1998. **431**(1-2): p. 79-96.
69. Benedetti, E., *X-ray crystallography of peptides: the contributions of the Italian laboratories.* Biopolymers, 1996. **40**(1): p. 3-44.
70. Hill, D.J., et al., *A field guide to foldamers.* Chem Rev, 2001. **101**(12): p. 3893-4012.
71. DeGrado, W.F., J.P. Schneider, and Y. Hamuro, *The twists and turns of beta-peptides.* Journal Of Peptide Research, 1999. **54**(3): p. 206-217.
72. Fisk, J.D., D.R. Powell, and S.H. Gellman, *Control of hairpin formation via proline configuration in parallel beta-sheet model systems.* Journal Of The American Chemical Society, 2000. **122**(23): p. 5443-5447.
73. Haque, T.S., J.C. Little, and S.H. Gellman, *Stereochemical requirements for beta-hairpin formation: Model studies with four-residue peptides and depsipeptides.* Journal Of The American Chemical Society, 1996. **118**(29): p. 6975-6985.
74. Haque, T.S., J.C. Little, and S.H. Gellman, *Mirror-Image Reverse Turns Promote Beta-Hairpin Formation.* Journal Of The American Chemical Society, 1994. **116**(9): p. 4105-4106.
75. Imperiali, B., et al., *A Conformational Study Of Peptides With The General Structure Ac-L-Xaa-Pro-D-Xaa-L-Xaa-Nh2 - Spectroscopic Evidence For A Peptide With Significant Beta-Turn Character In Water And In Dimethyl-Sulfoxide.* Journal Of The American Chemical Society, 1992. **114**(9): p. 3182-3188.